

1 **Short title:** Role of Trxs in the light-responsive redoxome

2

3 **Corresponding author:**

4 Prof. Dr. Peter Geigenberger

5 Address: Ludwig-Maximilians-University Munich, Department Biology I, 82152 Planegg-

6 Martinsried, Germany

7 Tel/Fax: +49 (089) 2180 74710 / +49 (089) 2180 74599

8 E-mail: geigenberger@biologie.uni-muenchen.de

9

10 **The impact of light and thioredoxins on the plant thiol-disulfide proteome**

11

12 Liang-Yu Hou, Frederik Sommer, Louis Poeker, Dejan Dziubek, Michael Schroda, Peter
13 Geigenberger*

14

15 Ludwig-Maximilians-University Munich, Department Biology I, 82152 Planegg-Martinsried,
16 Germany (L.-Y. H., L.P., D.D., P.G.); TU Kaiserslautern, Molekulare Biotechnologie und
17 Systembiologie, 67663 Kaiserslautern, Germany (F.S., M.S.); Academia Sinica, Institute of
18 Plant and Microbial Biology, 11529, Taipei, Taiwan (L.-Y. H.)

19

20 One sentence summary:

21 The plant protein redoxome shows light-dependent reduction and reoxidation dynamics
22 linked to Trxs *f1/f2*, *m1/m2* and NTRC, being of different importance depending on the
23 extent of light variability.

24

25 Footnotes:

26

27 P.G. conceived the project; L. -Y.H. and P.G. designed the research; L. -Y.H. F.S. and M.S.
28 performed the omics experiments; L.P. and D.D. assayed the protein redox states; L. -Y.H.
29 and P.G. analyzed the data; M.S. and P.G. supervised the experiments; L. -Y.H. and P.G.
30 wrote the manuscript.

31

32 This work was supported by the Deutsche Forschungsgemeinschaft (TRR175).

33

34 The author responsible for distribution of materials integral to the findings presented in this
35 article in accordance with the policy described in the Instructions for Authors
36 (www.plantphysiol.org) is: Peter Geigenberger (geigenberger@biologie.uni-muenchen.de)

37

38 Address correspondence to Peter Geigenberger (geigenberger@biologie.uni-muenchen.de)
39 and Liang-Yu Hou (a090716@icloud.com)

40

41 **Abstract**

42 Thiol-based redox regulation is a crucial post-translational mechanism to acclimate
43 plants to changing light availability. Here, we conduct a biotin-switch-based redox
44 proteomics study to systematically investigate dynamics of the thiol-redox network in
45 response to temporal changes in light availability and across genotypes lacking parts of the
46 thioredoxin (Trx) or NADPH-Trx-reductase C (NTRC) systems in the chloroplast. Time-
47 resolved dynamics revealed light leading to marked decreases in the oxidation states of many
48 chloroplast proteins with photosynthetic functions during the first 10 min, followed by their
49 partial re-oxidation after 2-6 hours into the photoperiod. This involved *f*, *m* and *x*-type Trx
50 proteins showing similar light-induced reduction-oxidation dynamics, while NTRC, 2-Cys-
51 Prx and Trx *y2* showed an opposing pattern, being more oxidized in the light than the dark. In
52 *Arabidopsis trxf1f2*, *trxm1m2* or *ntrc* mutants, in the light most proteins showed increased
53 oxidation states than wild type, suggesting their light-dependent dynamics being related to
54 the NTRC/Trx networks. While NTRC deficiency had a strong influence in all light
55 conditions, deficiencies in *f*- or *m*-type Trxs showed differential impacts on the thiol-redox
56 proteome depending on the light environment, being higher in constant or fluctuating light,
57 respectively. Results indicate plant redox proteomes to be subject to dynamic changes in
58 reductive and oxidative pathways to cooperatively fine-tune photosynthetic and metabolic
59 processes in the light. This involves *f*-type Trxs and NTRC to play a role in constant medium
60 light, while both *m*-type Trxs and NTRC being important to balance changes in protein
61 redox-pattern during dynamic alterations in fluctuating light intensities.

62

63 **Key words:** Thiol-based redox regulation, NADPH thioredoxin reductase, plastidial
64 thioredoxin, redox proteomics, light acclimation

65

66 **Introduction**

67 Due to their sessile lifestyle, plants experience countless environmental challenges.
68 Among these environmental stimuli, light availability is probably the most crucial factor,
69 since plants rely on photosynthesis to sustain their development and growth. In nature, the
70 fluctuations of light availability occur on a time-scale of seconds to months and encompass
71 large changes in irradiance. As sessile organisms, plants have evolved sophisticated strategies
72 to rapidly acclimate to frequently changed light intensities. While proteomics studies show
73 that there are only very minor changes in the abundance of proteins in response to fluctuating
74 light (FL; Niedermaier et al., 2020) or during diurnal changes in light availability (Uhrig et al.,
75 2021), the core of these regulatory mechanisms to rapidly acclimate light fluctuations is thiol-
76 based redox regulation of proteins. This kind of redox regulation exclusively occurs at thiol
77 groups of cysteine residues, which further changes protein activity and conformation
78 (Cremers and Jakob, 2013). The reactions of such disulfide-dithiol interchange rely on a
79 group of proteins called thioredoxins (Trxs; Meyer et al., 2012).

80 Thioredoxins are 12-14 kDa proteins harboring a conserved active site, WCGPC
81 (Holmgren, 1995). Trxs usually serve as disulfide reductase to reduce and activate their target
82 enzymes using NADPH via the mediation of NADPH-dependent Trx reductase (NTR)
83 proteins (Jacquot et al., 2009). In heterotrophic organisms, there are usually one or two genes
84 encoding Trx and NTR proteins in governing numerous redox regulations (Meyer et al.,
85 2012). Intriguingly, autotrophic organisms have rather complicated redox networks. For
86 example, cyanobacteria, algae and plants usually constitute a great number of Trx and NTR
87 proteins (Geigenberger et al., 2017; Zaffagnini et al., 2019). Unlike Trx proteins of
88 heterotrophic organisms exclusively gaining reducing power from NTR proteins, the
89 chloroplastic Trxs of autotrophic organisms can also drain reducing equivalents from
90 photosynthetically reduced ferredoxin (Fdx) with the involvement of Fdx-dependent Trx
91 reductase (FTR) proteins (Schürmann and Buchanan, 2008). In Arabidopsis, there are twenty
92 Trxs distributed in different subcellular compartments (Geigenberger et al., 2017; Zaffagnini
93 et al., 2019). Among these Trx proteins, the chloroplastic Trxs are of great importance for
94 chloroplast metabolism and light acclimation. With analyses in Trx mutant lines, the *f*-type
95 Trxs were determined as positive regulators for light-dependent carbon fixation, specifically
96 during dark-light transitions (Michelet et al., 2013; Thormählen et al., 2013; Thormählen et
97 al., 2015; Naranjo et al., 2016a). The *m*-type Trxs were found to regulate the redox state of
98 NADP-dependent malate dehydrogenase (NADP-MDH) to modulate the shuttle of reducing
99 equivalents via the malate valve (Okegawa and Motohashi, 2015; Thormählen et al., 2017;
100 Selinski and Scheibe, 2019). The *x*-type and *y*-type Trxs were found to be involved in

101 antioxidation processes (Collin et al., 2004; Lamkemeyer et al., 2006; Navrot et al., 2006;
102 Bohrer et al., 2012), while the α -type Trx was proposed to regulate plastidial gene expression
103 (Arsova et al., 2010).

104 In addition to the Fdx-Trx system, which is directly linked to light, a unique NTR
105 protein (NTRC) with joint Trx domain at its C-terminal end was discovered to use NADPH
106 to reduce the hydrogen peroxide scavenging enzyme 2-Cys peroxiredoxin (2-Cys Prx) in the
107 chloroplast (Serrato et al., 2004). Interestingly, NTRC was also found to affect broad
108 chloroplast metabolism, including the redox states of plastidial Trx targets (Serrato et al.,
109 2004; Michalska et al., 2009; Lepistö et al., 2013; Richter et al., 2013; Pérez-Ruiz et al., 2014;
110 Thormählen et al., 2015; Carrillo et al., 2016; Naranjo et al., 2016b; Da et al., 2017). These
111 effects were shown to be mainly indirect, with the redox balance of 2-Cys Prx indirectly
112 modulating Trx-regulated enzymes (Pérez-Ruiz et al., 2017; Cejudo et al., 2019; Cejudo et al.,
113 2021; Lampl et al., 2022). However, a comprehensive analysis of the redox proteome to
114 investigate the roles of NTRC and Fdx-Trxs in more detail remains to be studied.

115 To further resolve the Trx-mediated redox network, identifying the downstream
116 targets of Trxs became a much-anticipated research topic. Over the past two decades,
117 researchers have made a great effort on identifying Trx-target proteins. The initial approach
118 to pinpoint Trx targets relies on the basis of disulfide-dithiol interchange taking place
119 between Trx and its target protein. It has been established that the N-terminal cysteine of Trx
120 active site first reacts with the disulfide bond of the target protein, leading to the formation of
121 a transient heterodimer. The C-terminal cysteine of Trx active site subsequently initiates a
122 second reaction at the target disulfide bond to resolve this heterodimer. Afterward, the
123 oxidized Trx and the reduced target protein are further dissociated (Brandes et al., 1993;
124 Holmgren, 1995). Therefore, substitution of the C-terminal active cysteine to another amino
125 acid will disrupt the dissociation between Trx and its target, stabilizing the heterodimer. This
126 monocysteinic Trx variant can serve as bait to pull down its interacting targets. Such
127 technique together with two-dimensional gel electrophoresis has been extensively applied to
128 isolate Trx targets in cyanobacteria (Lindahl and Florencio, 2003; Pérez-Pérez et al., 2006),
129 Chlamydomonas (Goyer et al., 2002; Lemaire et al., 2004) and many land plants (Balmer et
130 al., 2003; Balmer et al., 2004b; Balmer et al., 2004a; Wong et al., 2004; Yamazaki et al.,
131 2004; Marchand et al., 2006; Bartsch et al., 2008; Montrichard et al., 2009; Marchand et al.,
132 2010; Yoshida et al., 2013) *in vitro*. Indeed, these studies identified hundreds of potential Trx
133 target proteins that require further confirmation and evaluation, specifically to demonstrate
134 their importance *in vivo* or to exclude unspecific binding due to Trxs acting as chaperones.

135 Another commonly used approach to identify Trx targets is to label the thiol group of
136 cysteine using a redox-active probe (Yano et al., 2001; Balmer et al., 2006; Alkhalfioui et al.,
137 2007; Hall et al., 2010). In addition to the qualitative application, several quantitative
138 modifications of this strategy such as biotinylated iodoacetamide (BIAM) switch assay and
139 an integrative proteomics method using cysteine-reactive isobaric tandem mass tags
140 (CysTMT, iTRAQ) differential cysteine labeling in combination with gel shifts were also
141 implemented to evaluate changes in the thiol redox status of proteins in various conditions
142 (Parker et al., 2015; Pérez-Pérez et al., 2017; Löwe et al., 2019; Zimmer et al., 2021).

143 Although a wide variety of redox proteomics approaches have been well developed, a
144 quantitative analysis of the thiol-disulfide redox proteome in response to different light
145 intensities is somewhat scarce. In the current study, we implemented the biotin switch assay
146 together with label-free quantification to evaluate the relative changes of protein oxidation
147 levels at different time points into the photoperiod and during fluctuating light intensities in
148 Arabidopsis plants. To further investigate the impact of the chloroplast thiol-redox network
149 on changes in protein oxidation levels during light acclimation, we analyzed several well-
150 characterized Trx mutants including *trxf1f2* (Naranjo et al., 2016a) and *trxm1m2* double
151 mutants (Thormählen et al., 2017) as well as the *ntrc* single mutant (Serrato et al., 2004) in
152 comparison to the wild type. By investigating light-dependent dynamics in the protein
153 redoxome, we demonstrated that large sets of proteins involved in photosynthetic light
154 reactions, Calvin Benson Cycle (CBC) and carbohydrate metabolism are reduced within 10
155 minutes of illumination, while they are subject to re-oxidation processes after 2-6 h into the
156 light period. Interestingly, *f*, *m* and *x*-type Trx proteins showed similar light-induced
157 reduction-oxidation dynamics as their photosynthetic targets, while NTRC, 2-Cys-Prx and
158 Trx *y2* showed an opposing pattern, being more oxidized in the light, compared to the dark.
159 Through studying the protein redoxome in the mutant lines deficient in parts of the thiol-
160 disulfide system, we uncovered that light-dependent *f*- and *m*-type Trxs play distinct roles in
161 modulating protein oxidation states in different light conditions. While Trxs *f1/f2* are more
162 important during regular growth light and in the high-light phases of fluctuating light (FL),
163 Trxs *m1/m2* mainly play a role during the low-light FL phases. In contrast, NTRC was found
164 to be indispensable to modulate the oxidation-state of photosynthetic proteins in all light
165 conditions, probably due to its role to regulate oxidative signals depending on NADPH. In
166 addition to well-known photosynthetic targets, we also identified proteins involved in
167 antioxidation processes and metabolism of amino acids and proteins to be subject to light-and
168 Trx-dependent redox modulation.

169

170 **Results**

171 **Light leads to temporal and spatial dynamics of the leaf redox proteome involving** 172 **mainly proteins with photosynthetic functions located in the plastid**

173 To understand effects of illumination on leaf protein redox states, we performed a
174 time-resolved study in the wild type. The design of this experiment is outlined in
175 Supplemental Figure S1A. Arabidopsis plants were grown under medium light intensity (ML,
176 $150 \mu\text{mol photons m}^{-2} \text{ s}^{-1}$ with a 12-h-dark/12-h-light regime; 22°C) for four weeks, before
177 leaf samples were harvested at different diurnal time points by freezing whole rosettes
178 directly into liquid nitrogen. We first harvested leaf samples at the end of the night (EN, dark
179 conditions), which served as the control. The following time points were 10 min (L10), 120
180 min (L120) and 360 min (L360) into the photoperiod, representing the effects of short, mid
181 and long-term illumination (Supplemental Fig. S1A). To analyze proteins that show light-
182 dependent changes in their oxidation states, leaf samples were subsequently subjected to a
183 redox-proteomics method, which is described in Supplemental Figure S1B. After protein
184 extraction in the presence of N-ethylmaleimide (NEM) to alkylate (and block) the free thiol
185 residues of cysteines, oxidized disulfides were subsequently reduced by DTT treatment, and
186 the resulting free thiol residues labeled with a redox-active biotin. The biotinylated proteins
187 were further isolated using a streptavidin resin, while mass spectrometry was used for protein
188 identification and quantification (Supplemental Fig. S1B). It must be noted, as we used NEM
189 to alkylate free thiol residues, our method mainly detected proteins subject to disulfide rather
190 than sulfenic acid modifications.

191 Using this approach, we successfully identified 1980 proteins which showed light-
192 induced changes in their oxidation states. Subsequently, proteins that have been detected in
193 less than three biological replicates were considered as low-abundance targets, and omitted
194 from the following data processing, as these identified targets were not valid for statistical
195 analyses. Then the remaining 1038 proteins were subjected to statistical analyses in
196 comparison to the EN (dark) samples. To do this, we calculated the fold changes of oxidation
197 levels between illuminated and dark samples to evaluate the effects of illumination on protein
198 oxidation states. Furthermore, we performed ANOVA with Dunnett's test, which yields a
199 probability value (P-value) to determine if the changes are statistically significant. Using
200 these criteria, 319 proteins were finally identified to harbor statistically significant ($P < 0.05$)
201 changes in oxidation states in response to illumination and selected for the following analyses
202 (Supplemental Table S1).

203 Because our approach only detects the oxidized forms of the proteins, but not their
204 reduction levels, calculation of absolute reduction/oxidation ratios was not feasible. We

205 therefore calculated the protein oxidation states at different time points into the photoperiod
206 relative to EN conditions. This approach is subject to possible errors, if there are
207 simultaneous changes in overall protein abundance during the dark-to-light transients.
208 However, a comprehensive proteomics study in Arabidopsis during the diurnal cycle showed
209 that only around 6% of the quantified proteome revealed marked changes in abundance over
210 the course of a day (Uhrig et al., 2021). By comparing the proteins identified in our present
211 study (Supplemental Table S1) with the published data set of Uhrig et al. (2021), we found
212 that only very few of the proteins that were identified to be subject to changes in oxidation
213 levels (16 out of 319) were also reported to be subject to diurnal changes in overall protein
214 levels (Supplemental Table S2). These 16 proteins listed in Table S2 were not in the focus of
215 our study. Overall this shows that, compared to redox alterations, protein abundance changes
216 are of minor importance under these conditions. Our approach is therefore appropriate to
217 evaluate dark-to-light changes in protein redox states during a time course of minutes to
218 hours.

219 To get a first overview, we grouped the 319 proteins according to their subcellular
220 localization and biological functions (Supplemental Table S1). As shown in Figure 1A,
221 around 39% of identified proteins are localized in the plastid; 21% in the cytosol and 9% in
222 mitochondria, while 31% are distributed to various other subcellular compartments. When
223 looking at their annotated functions, 13% of identified proteins are involved in
224 photosynthesis, 4% in cellular respiration, 10% in various other metabolic processes (e.g.,
225 carbohydrate, amino acid, lipid metabolism) and 7% in redox homeostasis. Interestingly, a
226 majority of 19% of identified proteins is involved in RNA and protein processes. The rest
227 (47% of identified proteins) are allocated to the group of other cellular processes and
228 unknown function (Figure 1B).

229 To further evaluate light-dependent effects on protein redox states, we performed a
230 principal component analysis (PCA). Results show that the L10 samples were clearly
231 deviated from the EN (dark) samples, while L120 and L360 samples showed a progressive
232 overlap with EN (Fig. 1C). This indicates that protein oxidation states changed dramatically
233 within the first 10 min of illumination, followed by a partial recovery at later time points. The
234 latter increased progressively with time, being more complete after 360, compared to 120 min
235 of illumination (Fig. 1C). The Venn diagram (Fig. 1D) shows the number of proteins with
236 different redox states after different time points of illumination, compared to EN (dark)
237 conditions. The non-overlapping regions of L10, L120 and L360 sample sets comprised 24%,
238 37% and 7% of the 319 proteins showing differential oxidation states, respectively. The
239 overlapping region between L10 and L120 comprised 18% of total identified targets,

240 indicating that the changes of oxidation state in these proteins endure in the short and
241 medium-term illumination. Rather few targets located in the overlapping region between
242 L360 and L10 (3% of total) as well as L360 and L120 (4% of total) suggesting that the
243 effects of longer-term light exposure on protein redox states are relatively minor when
244 compared to short-term and medium-term illumination (Figure 1D). It is worth noting that
245 there were 27 proteins (8% of total) displaying significant redox changes in all three time
246 points of illumination compared to EN (dark), including Calvin-cycle protein 12 (CP12),
247 NADP-dependent malate dehydrogenase (MDH) and POSTILLUMINATION
248 CHLOROPHYLL FLUORESCENCE INCREASE (PIFI). In these proteins, light-induced
249 changes in the oxidation status were maintained independent of the duration of illumination
250 (Supplemental Table S3).

251 To further visualize the redox patterns of identified targets, we conducted an
252 unsupervised cluster analysis. The 319 target proteins showing significant changes in redox
253 state were categorized into four clusters. Clusters 1 and 3 contained the targets showing a
254 strong increase in oxidation within the first 10 min (cluster 3) or 2 h of light exposure (cluster
255 1), while there was a partial re-reduction at later time points (Fig. 1, E and G). These mainly
256 included proteins located outside the plastid (Fig. 1I) and involved in functional categories
257 outside of photosynthesis, such as other metabolic processes, redox-homeostasis and
258 RNA/protein processes (Fig. 1J). Targets in clusters 2 and 4 instead showed an opposite
259 pattern, with proteins getting strongly reduced within 10 min (cluster 4) or 2 h upon
260 illumination (cluster 2), while they underwent some re-oxidation at later time points (Fig. 1, F
261 and H). Notably, most plastidial targets (Fig. 1I) and proteins involved in photosynthetic
262 processes were categorized to clusters 2 and 4 (Fig. 1J), the percentage of these proteins
263 being highest in cluster 4 (Fig. 1, I and J). This implies that a large part of plastidial proteins,
264 especially those participating in photosynthesis, becomes reduced within the first 10 min of
265 light exposure, as a possible “kick off” signal to activate photosynthetic processes. A partial
266 re-oxidation occurs at later time points, specifically after 360 min, indicating that during
267 long-term light exposure oxidative processes come into play.

268

269 **Light leads to a rapid increase in the reduction of proteins associated to photosynthesis** 270 **followed by their partial re-oxidation at later time points**

271 To in-depth understand the effects of light exposure on protein oxidation states in the
272 wild type, we categorized the targets showing significant changes into more detailed
273 functional groups and evaluated their protein oxidation levels (Fig. 2). Within the first 10 min,
274 light led to a rapid decrease in oxidation levels of almost all identified proteins involved in

275 photosynthetic light reactions (Fig. 2A), CBC (Fig. 2B) and major CHO metabolism (Fig.
276 2C). As shown in Figure 2A, 2B and 2C, these included 20 proteins of light reactions (i.e.
277 subunits of ATP-synthase, PSI and PSII reaction center, Chl a-b binding proteins, NDH, PIFI
278 and protein curvature thylakoid 1 B), 14 proteins associated to key steps of the CBC, and 19
279 proteins of major CHO metabolism, specifically starch and hexose-phosphate metabolism.
280 Intriguingly, only two target proteins listed within these categories, PsbP domain-containing
281 protein 6 (PPD6) and root isoform of FNR (RFNR1) behaved in an opposing manner, being
282 oxidized upon illumination, instead of being reduced (Fig. 2C), the RFNR1 being not directly
283 involved in photosynthetic metabolism. It is worth noting that RFNR harbors opposite
284 properties compared to LFNR. RFNR uses NADPH derived from the oxidative pentose
285 phosphate pathway (OPPP) to reduce Fdx, which further offers reducing equivalents to the
286 enzymes involved in nitrogen metabolism (Hanke et al., 2005). Thus, the oxidation of
287 RFNR1 might contribute to the active transferring of reducing power to Fdx and downstream
288 enzymes. These results reveal a whole set of photosynthetic proteins related to light reaction,
289 CBC and major CHO metabolism being subject to rapid light-dependent reduction. Indeed,
290 all identified proteins associated to the CBC showed a marked light-dependent decrease in
291 oxidation state within the first 10 min of illumination (Fig. 2B), which most likely involves
292 the Fdx-Trx system (Schürmann and Buchanan, 2008; Yoshida et al., 2022). In confirmation
293 of this, as indicated in Figure 2, all CBC proteins and a large part of the identified proteins
294 associated to light reactions and plastidial CHO metabolism have been reported as Trx targets
295 in previous studies (Lindahl and Kieselbach, 2009).

296 While the oxidation states of these photosynthetic proteins stayed low for up to 2 h in
297 the light, they surprisingly showed increasing re-oxidation after 6 h of illumination (Fig. 2, A,
298 B and C). This indicates that after several hours of light exposure also oxidative processes
299 come into play, leading to inactivation of a large set of photosynthetic proteins. Interestingly,
300 CP12-1 and CP12-2, involved in regulatory-complex formation with phosphoribulokinase
301 (PRK) and glyceraldehyde-3-phosphate dehydrogenase (GAPDH) in the CBC, showed
302 specifically strong decreases in their oxidation levels after 10 min light, while there was no
303 substantial re-oxidation at later time points, indicating both CP12 proteins to be less sensitive
304 to light-dependent oxidation processes in the chloroplast.

305 To directly verify our redox proteomics results by an independent method, we
306 selected three target proteins, namely plastidial fructose 1,6-bisphosphatase (CFBP),
307 glyceraldehyde-3-phosphate dehydrogenase B (GAPB) and PRK, to be analyzed by protein
308 electrophoretic mobility shift assay to assess light-dependent kinetics of their redox states
309 using the same plant material taken for redox proteomics. The reduced thiols of proteins were

310 alkylated using NEM, and the oxidized thiols of proteins were released by treating with DTT.
311 The released thiols were further labeled with methoxypolyethylene glycol maleimide, which
312 resulted in an increase of protein mass of the oxidized form, so that it became distinguishable
313 from the reduced form during gel-electrophoresis. After immunoblotting, the intensity of the
314 oxidized form was divided by the intensity sum of oxidized and reduced forms to yield the
315 oxidation percentage of the respective protein. The gel blots in Supplemental Figure S2 show
316 that all three proteins were fully oxidized in the dark (EN) yielding oxidation percentages of
317 100 % as shown in Figure 3. Compared to EN (dark), the oxidation percentages of CFBP and
318 GAPB dropped down in the first 10 min to around 30% and continued to decrease within the
319 next 2 h, while they showed subsequent re-oxidation after 6 h of light exposure
320 (Supplemental Figure S2 and Fig. 3). The oxidation percentage of the PRK protein decreased
321 very strongly already after 10 min of illumination down to levels that were hardly detectable,
322 showing that this protein was very efficiently reduced by the dark-to-light transition
323 (Supplemental Figure S2 and Fig. 3). These results obtained by gel-shift assays as an
324 independent method are in confirmation with the redox proteomics data, with the light-
325 dependent changes of the redox states of CFBP, GAPB and PRK being highly corresponding
326 between the two different methods (compare Fig. 3 and Fig. 2B). Overall, these results
327 validate our redox-proteomics data and the reliability of our experiment by an independent
328 method, indicating that the redox-proteomics method we are using here is appropriate to
329 determine light-dependent dynamics in protein redox states.

330

331 **Light leads to a more complex pattern of redox changes in proteins involved in redox** 332 **regulation, (photo)respiration, and protein metabolism**

333 While protein redox changes are most likely linked to cellular Trx systems (Baumann
334 and Juttner, 2002; Meyer et al., 2005; Geigenberger et al., 2017; Kang et al., 2019), light-
335 dependent redox dynamics of Trx proteins were also analyzed (Fig. 2, D and E). Chloroplasts
336 contain two different Trx systems, the Fdx/Trx system which is directly linked to light and
337 proposed to activate photosynthetic target enzymes, and the NTRC system which is linked to
338 NADPH and proposed as the major system to donate electrons to 2-Cys-Prx to convert H₂O₂
339 to H₂O (Zaffagnini et al., 2019). Fdx-dependent chloroplast Trxs such as Trxs *f1*, *f2*, *m1*, *m2*,
340 *m4* and *x* showed a rapid decrease in their oxidation states within the first 10 min, followed
341 by a re-increase after 120 and 360 min of light exposure (Fig. 2D), showing similar light-
342 induced reduction-oxidation dynamics as their photosynthetic targets (Fig. 2B). This suggests
343 *f*-, *m*- and *x*-types of Trxs to be subject to two opposing redox processes, leading to their
344 reduction and re-oxidation in the light. While reduction is most-likely mediated by photo-

345 reduced Fdx via FTR, acting within seconds to minutes of light exposure (Wang et al., 2014;
346 Yoshida et al. 2022), the nature of the re-oxidation processes in the light is more obscure, but
347 may be connected to 2-Cys peroxiredoxins (2-Cys Prxs; Lampl et al., 2022).

348 In comparison to this, both NADPH-dependent NTRC and Fdx-dependent Trx γ 2
349 showed an opposing pattern, being oxidized in the light, compared to the dark (Fig. 2D).
350 NTRC (Kirchsteiger et al., 2009; Cejudo et al., 2012; Pérez-Ruiz et al., 2017) and Trx γ 2
351 (Collin et al., 2004; Shin et al., 2020) have been proposed in previous studies to act as
352 efficient electron donors to 2-Cys Prx and Prx Q, respectively, to decompose H₂O₂ to H₂O.
353 Interaction of Trx γ 2 with 2-Cys Prx has also been demonstrated in a further study (Jurado-
354 Flores et al., 2020), suggesting Trx γ 2 to be involved in re-oxidation processes related to the
355 2-Cys-Prx system. Interestingly, chloroplast 2-Cys Prxs and Prx-IIE showed similar light-
356 dependent increases in their oxidation states, compared to NTRC and Trx γ 2 (Fig. 2, D and
357 E). In addition to this, chloroplast superoxide dismutase 2 (CSD2) involved in antioxidative
358 function showed an even stronger rise in its oxidation state upon illumination (Fig. 2E). The
359 light-induced increase in oxidation of this set of proteins is most likely due to increased
360 peroxide and ROS production during active photosynthetic processes in the chloroplast. This
361 contrasts with other chloroplast antioxidative proteins, such as FSD1, MDAR6, GSH1 and
362 APX4, and NAD(P)-dependent MDH, showing decreases in their oxidation states upon light
363 exposure, similar to photosynthetic enzymes (Fig. 2E). This confirms previous studies,
364 showing light-dependent reductive activation of NADP-MDH involved in the export of
365 reducing equivalents from the chloroplast (Scheibe, 1991).

366 Thioredoxins are also residing outside the chloroplast, where they are reduced by
367 NADP-dependent NTRA and NTRB (Reichheld et al., 2007; Bashandy et al., 2009; Cha et al.,
368 2014). Our data show that cytosolic (Trxs *h5* and *h3*) and mitochondrial (Trx *o1*) Trxs were
369 oxidized in response to light, as well as NTRA (Fig. 2D). However, oxidation of the latter
370 occurred only on a short-term basis (10 min light). Interestingly, with the exception of
371 monodehydroascorbate reductase (MDAR1) and GDP-mannose 3,5-epimerase (GME), extra-
372 plastidial glutathione peroxidases and reductases (GPX2, GPX6, GPX8 and ATGR1),
373 superoxide dismutase (CSD1) and Prx-IIF were oxidized in the light (Fig. 2E), showing a
374 similar pattern as extra-plastidial Trxs (Fig. 2D). Increased light-dependent oxidation of
375 extra-plastidial Trxs and related peroxidases is probably due to increased ROS and H₂O₂
376 production during photosynthesis.

377 We also identified light-dependent changes in oxidation states in several proteins
378 involved in photorespiration. Two peroxisomal enzymes, glycerate dehydrogenase (HPR) and
379 glycolate oxidase (GLO1), were markedly reduced, while two mitochondrial glycine

380 dehydrogenase proteins (GDH1 and GDH3) were oxidized during the day (Fig. 2F),
381 indicating illumination might trigger differential redox regulation for photorespiratory
382 processes in various subcellular compartments. When plants experienced a dark-to-light
383 transition, many proteins involved in amino acid metabolism were also subject to redox
384 changes (Fig. 2G). Notably, three plastidial enzymes showed strong redox changes during the
385 day. The aspartate aminotransferase (ASP5) and the Fdx-dependent glutamate synthase 1
386 (GLU1) underwent strong reduction upon illumination, while the NADH-dependent
387 glutamate synthase 1 (GLT1) showed an opposite redox pattern. In addition to this, we
388 identified a proposed redox-regulated enzyme, cysteine synthase (OASB; Lindahl and
389 Kieselbach, 2009), showing a strong reduction pattern during the day (Fig. 2G). It is worth
390 noting that three sulfur-assimilation-related enzymes, ATP sulfurylase (ATPS1, ATPS2 and
391 ATPS3), were significantly oxidized during the day (Fig. 2G), suggesting that also the sulfur
392 metabolism is redox-regulated in response to light.

393 Interestingly, targets involved in plastidial protein metabolism also displayed clear
394 redox changes during dark-to-light transition (Fig. 2H). These proteins were generally
395 reduced in response to light, except a 50S ribosomal protein (RPL13) and two peptide
396 methionine sulfoxide reductases (MSRB2 and MSR4). Notably, three of our identified targets
397 including the chloroplastic elongation factor (CPEFG), MSR4 and the protease (CLPP5),
398 were proposed to be redox-regulated targets in previous studies (Fig. 2H; Lindahl and
399 Kieselbach, 2009). This may indicate that light is modulating plastidial protein homeostasis
400 by redox regulation of a large set of target proteins in chloroplasts, confirming previous
401 results showing that global translation is subject to redox-regulation in Arabidopsis (Moore et
402 al., 2016) and yeast (Topf et al., 2018).

403

404 **Global changes of the redox proteome across mutants deficient in *m*-type Trxs, *f*-type** 405 **Trxs or NTRC under various light conditions**

406 Plastidial Trx proteins are crucial for light-dependent post-translational redox-
407 regulation of photosynthetic metabolism (Collin et al., 2003; Geigenberger et al., 2017; Kang
408 et al., 2019) and subject to reduction and oxidation in response to light-dependent processes
409 (see above). To obtain more insights into the role of the plastidial thiol-redox system to
410 regulate the cellular thiol-redox proteome, Arabidopsis mutants lacking parts of the Fdx-Trx
411 or NADPH-NTRC systems were analyzed. We selected mutants lacking *f*-type (*trxf1f2*) and
412 *m*-type Trxs (*trxm1m2*) as major and important parts of the chloroplast Fdx-Trx system, and
413 the *ntrc* mutant lacking NADPH-dependent NTRC in the plastid. All three T-DNA insertion
414 mutants have been extensively characterized in previous studies (Serrato et al., 2004; Naranjo

415 et al., 2016a; Thormählen et al., 2017). For confirmation, expression levels of the respective
416 genes were evaluated in these mutants, using real-time qPCR (Supplemental Fig. S3). As
417 expected, Trx *f1* and *f2* signals were undetectable in the *trxf1f2* double mutant, and no NtrC
418 signal was detected in the *ntrc* mutant, indicating both lines to be null mutants. In the
419 *trxm1m2* double mutant, no Trx *m1* signal was detected, while the expression of Trx *m2* was
420 decreased down to approx. 60% of wild-type levels. Plants were grown in two different light
421 conditions: In medium light (ML) as in the experiments described above, and in fluctuation
422 light (FL) consisting of rapidly alternating high light (HL) and low light (LL) phases of 1 and
423 5 min, respectively. To waive potential diurnal effects and focus on investigating the roles of
424 Trxs and NTRC in maintaining protein redox states, whole rosette leaves were harvested at
425 six hours into the photoperiod for redox proteomics analyses.

426 Through the biotin-switch approach, we successfully identified 2220 proteins with
427 redox-active Cys residues. After removing low-abundance targets (detected in less than 3
428 biological replicates) and subsequent statistical analyses (ANOVA with Dunnett's test), 772
429 proteins were selected for the following analyses, which showed significant changes ($P < 0.05$)
430 in their oxidation levels when compared to the wild-type (Supplemental Table S4). Since the
431 redox proteomics method used in this study does not provide absolute oxidation/reduction
432 ratios of proteins (see above) we calculated the protein oxidation states of the mutants
433 relative to the wild type. Data from a recent proteomics study indicate that this approach is
434 not subject to substantial errors with respect to changes in protein abundance. Indeed, in
435 constant ML or FL conditions, there were only minor changes in the overall abundance of
436 proteins in *trxf1*, *trxm1m2* and *ntrc* mutants, relative to wild type (Dziubek et al., 2023). A
437 comparison of our present data set (Supplemental Table S4) with those of Dziubek et al.,
438 (2023) pinpointed only 49 of the proteins that are relevant to the subsequent analyses and
439 shown in the following data displays to reveal significant changes in protein abundance in the
440 mutants relative to wild type (Supplemental Table S5). More crucially, as revealed in
441 Supplemental Table S5, these proteins showed only very minor changes in their quantified
442 levels (less than 3%) when mutants were compared to the wild type, indicating that changes
443 in protein expression levels can be neglected as possible errors in our study.

444 The identified targets were grouped according to their subcellular localization and
445 biological functions (Fig. 4, A and B). Most targets were localized in plastid (37% of total),
446 cytosol (25% of total) and mitochondria (9% of total), while the rest (29% of total) distributes
447 to other subcellular compartments (Figure 4A). As shown in Figure 4B, a large set of targets
448 was associated to photosynthesis (13% of total), cellular respiration (5% of total), metabolic
449 pathways (16% of total), redox homeostasis (5% of total) and RNA/protein processes (26%

450 of total), while those remaining (36% of total) were allocated to the group of other cellular
451 processes and unknown functions (Fig. 4B).

452 We further performed PCA to visualize the effects of various light conditions on
453 protein oxidation levels in different genotypes. In ML, the four genotypes formed four
454 different clusters. The cluster of the *trxf1f2* double mutant was close to the wild type (Col-0)
455 with a slight overlapping, while the clusters of *trxm1m2* and *ntrc* mutant lines stayed close to
456 each other but were clearly deviated from the clusters of Col-0 and *trxf1f2* (Fig. 4C). When
457 looking at the HL phases of FL, the clusters of *trxf1f2* and *ntrc* clearly deviated from the
458 wild-type cluster, while the cluster of *trxm1m2* was largely overlapping with the clusters of
459 Col-0 and *ntrc* (Fig. 4D). In the LL phases of FL, the *trxf1f2* double mutant clustered together
460 with the wild type, while both *trxm1m2* and *ntrc* clustered differently and clearly deviated
461 from the wild type (Fig. 4E). Taken together, these data indicate that *f*-type Trxs, *m*-type Trxs
462 and NTRC have differential effects on the redoxome in ML, while in FL, *f*-type Trxs have a
463 more specific effect on the redoxome in the HL phases, but *m*-type Trxs and NTRC in the LL
464 phases.

465 Furthermore, we used Venn diagrams to visualize specific mutant effects on protein
466 redox states in different light conditions. In ML, the *ntrc* mutants harbored 26% of identified
467 proteins showing marked changes in their oxidation levels with respect to the wild type,
468 suggesting a major role of NTRC in regulating global protein redox states, while the *trxf1f2*
469 and *trxm1m2* double mutants comprised only 14% and 13% of identified proteins,
470 respectively (Fig. 4F). Comparable amounts of targets resided in the overlapping region
471 between *trxf1f2* and *ntrc* (18% of total) as well as *trxm1m2* and *ntrc* mutant lines (15% of
472 total), indicating NTRC to influence the redox states of both *f* and *m*-type Trx target proteins,
473 most likely in an indirect manner (Pérez-Ruiz et al., 2017). Nevertheless, only 4% of
474 identified proteins were located in the overlapping region between *trxf1f2* and *trxm1m2*
475 mutants (Fig. 4F), indicating the target specificities of *f* and *m*-type Trxs being rather distinct.
476 Interestingly, there were 10% of identified proteins showing differential changes in their
477 oxidation states with respect to the wild type in either of *trxf1f2*, *trxm1m2* or *ntrc* mutant lines.

478 In FL, the *ntrc* mutant comprised the largest number of identified proteins showing
479 significant changes in their oxidation levels relative to the wild type, in both HL (26% of total;
480 Fig. 4G) and LL phases (31% of total; Fig. 4H). Interestingly, deficiencies of *f*-type Trxs led
481 to larger changes in protein redox states (24% of total) in the HL phases (Fig. 4G) than in the
482 LL phases (5% of total; Fig. 4H). This contrasts with deficiencies in *m*-type Trxs, which led
483 to larger effects in the LL phases (20% of total) than in the HL phases (14% of total) of FL
484 (Fig. 4H). The number of identified proteins residing in the overlapping regions between *ntrc*

485 and *trxm1m2* were higher than in those between *ntrc* and *trxf1f2*, specifically in the LL
486 phases (Fig. 4, G and H). This indicates a differential impact of *f*- and *m*-type Trxs on their
487 target proteins in the HL and LL phases of FL, reflecting the different influence of NTRC on
488 the redox states of these target proteins in the different light phases, which is mainly due to
489 indirect effects (Fig. 4, G and H). Similar to ML conditions (Fig. 4F), in both HL (Fig. 4G)
490 and LL phases of FL (Fig. 4H) only 4% of the identified proteins were located in the
491 overlapping region between *trxf1f2* and *trxm1m2* mutants, indicating very distinct target
492 specificities of *f*- and *m*-type Trxs independent of the light conditions.

493

494 **Deficiencies in *f*-type Trxs, *m*-type Trxs or NTRC differentially affect the redox** 495 **proteome of photosynthesis and carbohydrate metabolism dependent on the light** 496 **conditions**

497 To further understand the contribution of plastidial thioredoxins (pTrxs) on the global
498 redox proteome, we calculated the fold changes of protein oxidation levels in the mutant lines
499 with respect to the wild type and categorized the targets showing significant difference
500 (ANOVA with Dunnett's test) into more detailed functional groups (Supplemental Table S4).
501 In ML, deficiencies in *f*-, *m*-type Trxs or NTRC similarly led to a diverse pattern in the
502 oxidation levels of proteins of the different photosystems (Fig. 5, A and B). When looking at
503 the detailed changes of respective proteins, many PSI proteins became more oxidized, while
504 several oxygen evolving enhancer proteins and PSII proteins were getting reduced in the
505 *trxf1f2* mutants, compared to the wild type (Fig. 5, A and B). In comparison to the wild type,
506 deficiency of NTRC led to a diverse redox pattern on PSI proteins, while the changes of PSII
507 proteins in the *ntrc* mutant were similar to those in the *trxf1f2* mutant. In the *trxm1m2* double
508 mutant, a large set of PSII proteins became more oxidized compared to the wild type, while
509 the redox changes of PSI proteins were more diverse (Fig. 5, A and B). It is worth to note that
510 deficiencies of *f*-, *m*-type Trxs or NTRC led to a mild increase in oxidation pattern in most
511 electron carriers and ATP synthases except the cytochrome b6f proteins (PETA and PETC;
512 Fig. 5C).

513 In contrast to this, during FL, the *trx* and *ntrc* mutant lines displayed distinct redox
514 patterns in photosystem proteins. In the *trxf1f2* double mutant, the PSI proteins underwent
515 diverse and minor redox changes (Fig. 5A), while the PSII proteins showed a general
516 reduction pattern during the HL phases, compared to the wild type. Such reductive pattern
517 was mitigated during the LL phases (Fig. 5B). Deficiency of *ntrc* led to marked reduction in
518 most PSI proteins during either HL or LL phases. The redox patterns of PSI proteins in
519 *trxm1m2* mutants were similar to those in *ntrc* mutants during the HL phases, while such

520 reduction pattern was not maintained during the LL phases (Fig. 5A). When looking at the
521 PSII group, the *ntrc* mutants showed a reduction pattern in oxygen-evolving proteins, but an
522 oxidation pattern in other PSII reaction center proteins and chlorophyll-binding proteins,
523 compared to the wild type. Such redox changes became more significant in the *ntrc* mutants
524 during the LL phases (Fig. 5B). The redox patterns of PSII proteins in *trxm1m2* were similar
525 to those in *ntrc* mutants. It is worth noting that the *trxf1f2* mutants exhibited a consistent
526 reduction pattern on D1, CP47 and CP43 proteins (PSBA, PSBB and PSBC), while the
527 *trxm1m2* mutants displayed opposite redox patterns on these three targets. This suggests *f* and
528 *m*-type Trxs to be involved in an opposing manner in the assembly and repair of PSII. Indeed,
529 it has been proposed that the *m*-type Trxs play a role in the biogenesis of PSII (Wang et al.,
530 2013). Compromising *f*-type Trxs merely led to reduction of several ATP synthase proteins
531 compared to the wild type (Fig. 5C). Nevertheless, deficiencies in *m*-type Trxs or NTRC
532 similarly resulted in oxidation of most ATP synthase proteins during the HL phases, while
533 such redox changes became less significant during the LL phases (Fig. 5C). Interestingly, in
534 the *ntrc* mutants, the redox patterns of PETA and two ATP synthases (AT4G32260 and
535 ATPF) appeared to be opposite between HL and LL phases (Fig. 5C). Taken together, the
536 diverse redox changes of photosystem proteins in the different mutants indicate that different
537 types of Trxs differentially affect the redox state of proteins of the photosynthetic light
538 reactions.

539 Looking at enzymes of the CBC, deficiencies in Trxs *f1f2*, Trxs *m1/m2* or NTRC led
540 to increased oxidation states of the respective proteins (Fig. 5D). This is in line with previous
541 studies showing CBC enzymes to represent clear and confirmed targets of *f*- and *m*-type Trxs
542 with different affinities, (Lindahl and Kieselbach, 2009; Yoshida et al., 2015; McFarlane et
543 al., 2019; Yu et al., 2020), while the effect of NTRC on the redox state of these targets was
544 shown to be indirect (Ojeda et al., 2017; Pérez-Ruiz et al., 2017). Interestingly, there were
545 differences in the impact of these thiol-redox regulators on the redox-state of CBC targets
546 depending on the light conditions. In ML, deficiencies of *f*-type Trxs or NTRC resulted in
547 marked oxidation of almost all CBC proteins, while compromising *m*-type Trxs hardly
548 affected the oxidation states of these targets (Fig. 5D). In FL, a different situation emerged. In
549 the HL phases of FL, all three mutant lines displayed largely similar oxidation levels of CBC
550 proteins, except a reduction in CP12-1 in the *trxm1m2* double mutant. When shifted to the LL
551 phases, the redox states of most CBC enzymes remained oxidized in the *trxm1m2* and *ntrc*
552 mutant lines, while those of the *trxf1f2* mutants showed a re-reduction to wild-type levels
553 (Fig. 5D). While these results are in line with the generally accepted roles of Fdx-Trxs and
554 NADPH-NTRC to modulate the reduction and hence the activation state of CBC enzymes

555 (Michelet et al., 2013) they surprisingly show their different impacts depending on the light
556 conditions. Specifically, our results indicate different impacts of *f*-type and *m*-type Trxs in
557 reducing CBC enzymes in ML and FL conditions, with *m*-type Trxs playing a more important
558 role in FL than in ML, and *f*-type Trxs being more important in ML and HL, rather than LL.

559 Next, we looked at the group of major CHO metabolism in the plastid. In ML,
560 deficiencies of *f*-type Trxs led to a general oxidation of most CHO metabolism enzymes,
561 while compromising *m*-type Trxs had only very minor effects on the redox states of these
562 targets (Fig. 5E). Deficiency of NTRC resulted in diverse impacts on the redox states of CHO
563 metabolism enzymes: A set of starch degradation enzymes was more reduced, while the CHO
564 anabolic enzymes, including the well-known NTRC target, APS1, involved in starch
565 synthesis, were more oxidized in the *ntrc* mutants compared to the wild type (Fig. 5E). In FL,
566 no clear redox change of CHO metabolism enzymes was observed in the *trxf1f2* mutants.
567 Nevertheless, during the LL phases, compromising *m*-type Trxs or NTRC led to a general
568 oxidation in a large set of CHO metabolism enzymes (Fig. 5E). With respect to the redox
569 regulation of CHO enzymes, this indicates *f*-type Trxs to play a major role in ML, while *m*-
570 type Trxs appear to be more important in FL. Compromising NTRC led to increased
571 oxidation of CHO enzymes in all light conditions, suggesting a more general role of NTRC in
572 light regulation of carbohydrate metabolism. Notably, the RFNR1 was markedly reduced in
573 the *trxf1f2* and *ntrc* mutant lines compared to the wild type in ML, and such reduction pattern
574 was exacerbated only in the *trxf1f2* mutants during the HL phases of FL. Nevertheless, in the
575 *ntrc* mutants, the redox state of RFNR1 was not altered during the HL phases but became
576 more oxidized during the LL phases (Fig. 5E). Considering that the RFNR1 mediates the
577 electron transfer between oxidative pentose phosphate pathway (OPPP) and downstream
578 enzymes (Hanke et al., 2005), it is likely that the *f*-type Trxs and NTRC can regulate RFNR1
579 redox states to further modulate OPPP.

580 It has been reported that NTRC is involved in tetrapyrrole biosynthesis by regulating
581 magnesium chelatase (Richter et al., 2013). Indeed, the target proteins of tetrapyrrole
582 metabolism were more oxidized in the *ntrc* mutants compared to the wild type in ML,
583 confirming the positive role of NTRC in chlorophyll biosynthesis (Fig. 5F). In addition,
584 several targets of tetrapyrrole metabolism appeared to be more oxidized in the *trxf1f2* and
585 *trxm1m2* mutants compared to the wild type (Fig. 5F), indicating both *f* and *m*-type Trxs also
586 to participate in chlorophyll metabolism, as has been reported previously (Da et al., 2017;
587 Wittmann et al., 2023). Increased oxidation of these proteins was maintained in the HL
588 phases of FL, with some exceptions showing rather reduced status compared to the wild type
589 (Figure 5F). Notably, the protoporphyrinogen oxidase (PPOX1) was dramatically reduced in

590 the *trxf1f2* and *ntrc* mutant lines during the LL phases. Furthermore, the protochlorophyllide
591 reductases (PORB and PORC) and glutamyl-tRNA reductase (HEMA1) underwent reduction
592 exclusively in the *ntrc* mutants during the LL phases, compared to WT (Fig. 5F).

593

594 **Deficiencies in *f*-type Trxs, *m*-type Trxs or NTRC affect the oxidation states of proteins** 595 **involved in redox homeostasis, photorespiration, nitrogen and sulfur metabolism**

596 We also evaluated the role of Trxs to catalyze redox changes in proteins involved in
597 redox homeostasis. In ML, deficiencies of *f*-type Trxs or NTRC led to diverse redox changes
598 in plastidial targets, while lack of *m*-type Trxs hardly changed the redox states of most targets
599 (Fig. 6A) with the exception of superoxide dismutase [Fe] 1 (FSD1), which underwent
600 marked oxidation in the *trxm1m2* mutant, but significant reduction in the *ntrc* mutant.
601 Another superoxide dismutase [Cu-Zn] 2 (CSD2) and glutathione peroxidase (GPX1) were
602 greatly oxidized in the *ntrc* mutant (Fig. 6A). Moreover, compromising the *m/f*-type Trxs or
603 NTRC led to general reduction patterns in extra-plastidial targets including peroxiredoxins
604 and enzymes of ascorbate-glutathione (AsA-GSH) cycle (Fig. 6A). Interestingly, there were
605 changes in the redox pattern in the different phases of FL. In the HL phases, the different
606 mutants led to similar changes as in ML, with the exception that in the *ntrc* mutant, CSD2
607 and GPX1 were less oxidized, while FSD1, Fdx-Trx reductase (FTRC), peroxiredoxins, and
608 GSH S-transferase (DHA3) were more reduced, compared to the ML (Fig. 6A). This
609 contrasts with the LL phases, where a set of targets including malate dehydrogenase (NADP-
610 MDH), 2-Cys peroxiredoxin (BAS1), BAS1-like protein (2-Cys Prx B) and certain enzymes
611 of AsA-GSH cycle (APX4 and MDAR6) showed strongly increased oxidation states in the
612 *trxm1m2* and *ntrc* and mild increases in *trxf1f2* mutants, compared to HL phases of FL or ML
613 (Fig. 6A). These redox changes of NADP-MDH are in line with a previous study using
614 Arabidopsis mutants documenting that *m*-type Trxs and NTRC are involved in the activation
615 of plastidial NADP-MDH *in vivo* (Thormählen et al., 2017). In contrast to *m*-type Trxs,
616 NTRC is acting via an indirect mechanism, since it did not lead to a reduction of NADP-
617 MDH via direct interaction *in-vitro* (Delgado-Requerrey et al., 2023). Interestingly,
618 chloroplast NAD-MDH was slightly reduced, indicating that the oxidation states of NAD and
619 NADPH dependent MDHs located in the chloroplast responded differently after transfer from
620 ML to FL. Furthermore, FTRC protein involved in Trx reduction was strongly reduced in all
621 three mutant lines in FL, but not ML. With respect to the redox changes in extra-plastidial
622 targets involved in redox homeostasis in FL, compared to ML, there was a clear tendency to
623 increased oxidation states in most of the proteins in all three mutants. This was especially
624 marked in the LL phases of FL (Fig. 6A).

625 There is evidence for cross talk between NTRC, 2-Cys Prx and Trxs *f* (Pérez-Ruiz et
626 al., 2017) or Trxs *m* (Delgado-Requerey et al., 2023) in vivo. We thus investigated the redox
627 changes of the other types of Trxs and Trx reductases in the selected mutant lines (Fig. 6B).
628 In ML, deficiency of *f*-type Trxs elicited an increased reduction in Trx *m2* and a reduction
629 pattern in other Trxs, including plastidial Trxs *m1*, *m4*, *x* and NTRC as well as cytosolic Trxs
630 *h3* and *h5*, while the plastidial ACHT2 protein was more oxidized. Combined deficiencies of
631 Trxs *m1* and *m2* instead led to increased oxidation of Trxs *m3* and *m4* in the plastid, while
632 there was a decrease in the oxidation of extra-plastidial Trxs, specifically Trx *h3* and *h5*
633 proteins in the cytosol. In response to NTRC deficiency, surprisingly, the oxidation of all
634 other Trxs and Trx reductases was mitigated, except for cytosolic Trxs *h3* and *h5* showing
635 strong decreases in their oxidation states (Fig. 6B). In FL, all three different mutants showed
636 increased oxidation patterns in other Trxs and Trx reductases, when compared to ML (Fig.
637 6B). In the HL phases of FL, the rise in the oxidation states of those proteins was stronger
638 than in LL phases, while *ntrc* and *trxm1m2* mutants showed more increased oxidation states
639 than *trxf1f2* mutants, specifically with respect to the plastidial Trxs *f2*, *m3*, *m4*, *y2*, *x*, like-4,
640 and ACHT2, and all extra-plastidial Trxs (Trxs *h3*, *h5*, *o1* and NTRA). Taken together,
641 deficiencies in *f*, *m*-type Trxs or NTRC led to differential effects in the redox states of other
642 Trxs and Trx reductases dependent on the light conditions. While there were some mild
643 decreases in oxidation in ML, oxidation states of most of those proteins were strongly
644 increased in FL, specifically in the HL phases, with *ntrc* and *trxm1m2* having a much greater
645 impact than *trxf1f2* mutants. This shows that in FL environments, NTRC and Trxs *m1/m2* are
646 specifically important to keep the other types of Trxs in a reduced state, also outside the
647 plastid boundaries.

648 With respect to proteins of photorespiratory processes, all three mutants showed
649 increased oxidation states, compared to wild type (Fig. 6C). In ML, *trxf1f2* and *ntrc* mutants
650 showed the strongest effects on these photorespiratory targets, while in FL, specifically in the
651 LL phases the impacts of *trxm1m2* and *ntrc* were more marked than those of *trxf1f2*.
652 Interestingly, two glycine cleavage system proteins (GDH1 and GDH2) became less oxidized
653 in *trxm1m2* and *ntrc* mutants in ML, while they showed a strong increase in oxidation in all
654 three mutant lines in the LL phases of FL (Fig. 6C). Considering that most targets of
655 photorespiration reside outside plastids, it is unlikely that the pTrxs or NTRC can directly
656 modulate their redox states. Thus, the observed protein-redox changes are most likely the
657 result of inter-organelle redox transfer by mechanisms such as the malate valve.

658 Following a similar pattern, almost all enzymes involved in plastid nitrogen and sulfur
659 metabolism showed increased oxidation states in all mutants, compared to wild type (Fig.

660 6D). This involved several important enzymes such as sulfite reductase (SIR), glutamine
661 synthetase (GLN2), Fdx-dependent glutamine synthase 1 (GLU1) and aspartate
662 aminotransferase (ASP5), with SIR and GLN2 being suggested to be subject to redox-
663 regulation in previous studies (Lindahl and Kieselbach, 2009). In ML, the impacts of *trxf1f2*
664 and *ntrc* were stronger than those of *trxm1m2* mutants, while in the LL phases of FL, the
665 impacts of *trxm1m2* became more dominant, while those of *trxf1f2* became diminished. This
666 indicates *f*-, *m*-type Trxs and NTRC to be of general importance to keep the reduction states
667 of enzymes of nitrogen and sulfur metabolism in a reduced state to optimize their activities in
668 response to light. In this respect, the impacts of *f*-type and *m*-type Trxs were found to be
669 different depending on the light conditions, being higher in ML and LL phases of FL,
670 respectively.

671

672 **Deficiencies in *f*-type Trxs, *m*-type Trxs or NTRC affect the oxidation states of proteins** 673 **involved in secondary metabolic pathways and protein homeostasis**

674 We also looked at mutant effects on oxidation states of enzymes involved in other
675 metabolic processes, such as lipid, nucleotide and secondary metabolism. Overall the three
676 different mutants showed increased oxidation states of most of the proteins involved in these
677 pathways, when compared to wild type (Supplemental Fig. S4). This included key enzymes
678 of plastidial isoprenoid synthesis which have been suggested to be regulated by
679 thiol/disulfide modulation in previous studies (Supplemental Fig. S4; Lindahl and Kieselbach,
680 2009) and shown to be involved in the methylerythritol 4-phosphate (MEP) pathway (i.e., 1-
681 deoxy-D-xylulose 5-phosphate reductoisomerase, DXR; 4-hydroxy-3-methylbut-2-en-1-yl
682 diphosphate synthase and reductase, ISPG and ISPH) and in the xanthophyll cycle
683 (violaxanthin de-epoxidase, VDE1), where impacts of the different mutants on oxidation
684 states were strongly dependent on light conditions. While in ML the oxidation states of these
685 proteins were substantially increased, such oxidation patterns were mitigated in the HL
686 phases, while there was a strong re-increase in the LL phases of FL (Supplemental Fig. S4).
687 These dramatic changes in the oxidation pattern of these proteins between HL and LL phases
688 of FL occurred within 1-4 min and were specifically marked in *trxm1m2* and *ntrc* mutants.
689 This indicates that NTRC and Trxs *m1/m2* are specifically important to balance the redox
690 states of key enzymes of isoprenoid and zeaxanthin synthesis during rapidly altering HL and
691 LL. The impacts of NTRC and Trxs *m1/m2* were specifically strong with respect to VDE1,
692 the key enzyme of zeaxanthin synthesis, which is crucial to decrease the photochemical
693 efficiency of photosystem II by increasing heat dissipation via non-photochemical quenching
694 (NPQ) to allow photoprotection during HL stress (Hieber et al., 2000). In confirmation to this,

695 both, NTRC and Trxs *m1/m2* were found to affect NPQ in the HL phases of FL (Thormählen
696 et al., 2017).

697 Among the identified proteins, a surprisingly large set of targets involved RNA and
698 protein processes in the plastid (Fig. 4B). We therefore had a closer look on genotypic
699 changes in the oxidation states of these plastidial proteins (Supplemental Fig. S5). In ML, a
700 large set of 30S and 50S ribosomal proteins and the elongation factors TUFA, emb2726 and
701 CPEFG showed increases in their protein oxidation levels in all three mutant lines, compared
702 to the wild type (Supplemental Fig. S5). This involved also proteins which have been
703 suggested to be subject to thiol/disulfide regulation in previous studies (Supplemental Fig. S5;
704 Lindahl and Kieselbach, 2009). Compared to ML, the oxidation levels of most of these
705 proteins were found to be decreased in all three mutants in FL, specifically in the LL phases,
706 where a set of 50S ribosomal proteins displayed a marked decrease in their oxidation states
707 (Supplemental Fig. S5). Although deficiencies in *f*-, *m*-type Trxs or NTRC showed clear
708 impacts on the oxidation levels of these ribosomal proteins, whether such redox changes
709 affect protein metabolism requires further investigations.

710

711 Discussion

712 Previous proteomics studies showed light variability with respect to diurnal changes
713 (Uhrig et al., 2021) or fluctuating light (Niedermaier et al., 2020; Dziubek et al., 2023) to be
714 associated with only minor changes in the overall abundance of proteins, pointing to the
715 importance of thiol-disulfide modulation to regulate protein functions in response to light
716 changes. However, in this context, our knowledge on the light-dependent dynamics of the
717 plant redoxome is still scarce. In the present study, we performed biotin-switch based redox
718 proteomics to systemically investigate the dynamics of light-dependent plant thiol-redox
719 networks. By analyzing Arabidopsis plants at different time points into the photoperiod, we
720 revealed illumination to lead to a marked increase in the reduction of a large set of proteins
721 involved in photosynthetic processes during the first 10 min, followed by their partial re-
722 oxidation after 2-6 h. Interestingly, *f*, *m* and *x*-type Trx proteins showed similar light-induced
723 reduction-oxidation dynamics as their photosynthetic targets, while NTRC, 2-Cys-Prx and
724 Trx $\gamma 2$ showed an opposing pattern, being more oxidized in the light, compared to the dark.
725 This indicates the Trx/NTRC systems to be involved in, both, light-dependent reduction and
726 re-oxidation dynamics. By analyzing Arabidopsis *trxf1f2*, *trxm1m2* and *ntrc* mutants, we
727 found most protein targets to show increased oxidation states, compared to the wild type,
728 suggesting their light-dependent decreases in oxidation states to be related to Trxs.
729 Interestingly, *f*- and *m*-type Trxs were found to have different impacts on the thiol-redox

730 proteome depending on the light conditions, with the impacts of Trxs *f1/f2* to be higher in ML,
731 while those of Trxs *m1/m2* being increased in the LL-phases of FL. Compared to this, NTRC
732 was found to have a strong impact in all light conditions. This indicates *f*-type Trxs, *m*-type
733 Trxs and NTRC to be of general importance to keep the light-dependent thiol-redox proteome
734 in a reduced state to optimize the functions of the constituent proteins, while they show
735 different impacts depending on the light conditions.

736

737 **Light leads to reduction and re-oxidation dynamics of the plastid thiol-redox proteome**

738 Our redox proteomics study shows that proteins revealing significant light- and Trx-
739 dependent changes in their oxidation states were preferentially localized in the plastid (Fig.
740 1A and 4A) with photosynthesis being a major function (Fig. 1B and 4B). This is in
741 agreement with a previous study, investigating the differential redox-modified proteins
742 between regular growth light (GL) and FL in Arabidopsis, showing most proteins are
743 localized in chloroplasts (Chen et al., 2022). Moreover, another redox proteomics study
744 conducted in tobacco plants subjected to a very short-term dark-to-light transition also found
745 that the identified proteins with redox-regulated and light-responsive properties are mainly
746 localized in chloroplasts, even though the authors claimed their redox proteomics approach
747 may not be suitable for proteins with multiple redox forms (Zimmer et al., 2021).
748 Furthermore, a thioredoxome study in *Chlamydomonas* also found approx. 30% of 1188 Trx
749 targets reside in chloroplasts (Pérez-Pérez et al., 2017). Taken together, light-dependent
750 dynamics of the plant redox proteome are mainly localized to the chloroplast, where they are
751 subject to the Trx systems linked to photo-reduced Fdx and NADPH-dependent NTRC.

752 When light-dependent changes in our redox proteomics data were analyzed in more
753 detail, a large set of proteins involved in photosynthetic light reaction, CBC and carbohydrate
754 metabolism showed marked decreases in their oxidation states within 10 min of illumination,
755 compared to the dark (Fig. 2A). This observation is in line with the commonly accepted
756 notion suggesting that illumination induces a rapid reductive signal pathway to activate
757 chloroplast metabolism (Michelet et al., 2013). In confirmation to this, there was a rapid
758 decrease in the oxidation states of chloroplast Trxs of *f*-type, *m*-type and *x*-type (Fig. 2D),
759 which use electrons from photoreduced Fdx to reduce and activate plastidial targets.
760 Interestingly, although such reduction patterns sustained within the next 2 hours of light
761 exposure, oxidation levels increased again, returning almost to initial dark levels after six
762 hours of illumination, indicating the occurrence of re-oxidation dynamics later in the
763 photoperiod (Fig. 2, B and C; confirmed by an independent method in Fig. 3). This re-
764 oxidation pattern was accompanied by increased oxidation states of *f*-, *m*- and *x*-type Trxs

765 (Fig. 2D), which are probably attributable to an oxidation loop via 2-Cys-Prx (Zaffagnini et
766 al. 2019). Interestingly, our present data show that 2-Cys-Prx, NTRC and Trx γ 2 are oxidized
767 in the light, which supports this notion (Fig. 2, D and E).

768 Similar reduction and re-oxidation processes were previously documented when
769 investigating the redox changes of NADP(H) couples during the dark-to-light transition,
770 where the ratio of NADPH to the total pool of NADP+NADPH rapidly increased upon
771 illumination, while recovering to the dark level after merely 3 min of light (Heber and
772 Santarius, 1965; Dietz and Hell, 2015). Moreover, a recent study using biosensors to monitor
773 cellular redox signals revealed that the Fdx-mediated reductive signals interact with the 2-
774 Cys Prxs-mediated oxidative signals to fine-tune photosynthetic processes (Lampl et al.,
775 2022). In fact, deficiencies of 2-Cys Prxs were reported to facilitate the reduction of certain
776 CBC enzymes (Pérez-Ruiz et al., 2017). Moreover, co-incubating oxidized 2-Cys Prx with
777 plastidial Trxs can effectively inactivate CFBP and MDH activities (Vaseghi et al., 2018). In
778 this context, the light-dependent increase in H₂O₂ may account for the substantial oxidation
779 of 2-Cys Prxs and its electron donor, NTRC, during the day (Fig. 2, D and E), as both
780 components need to serve as electron sinks to maintain the oxidative signal transduction.
781 Moreover, oxidation of NTRC in the light may also be due to the reoxidation pattern of the
782 NADPH/NADP redox couple after 3 min of illumination (Heber and Santarius, 1965; Dietz
783 and Hell, 2015). The finding that NTRC is oxidized in the light is in line with its proposed
784 mechanism to act indirectly on plastidial targets via 2-Cys Prx (Pérez-Ruiz et al., 2017),
785 rather than by their direct reduction (Ojeda et al., 2017). Interestingly, also Trx γ 2 has been
786 proposed in previous studies to act as efficient electron donor to 2-Cys Prx (Collin et al.,
787 2004; Jurado-Flores et al., 2020; Shin et al., 2020), while it was shown to be inefficient to
788 directly reduce CBC proteins (Collin et al., 2004; Yoshida et al., 2015). The reason for this
789 unexpected specificity of Trx γ 2 remains to be determined. In summary, our redox
790 proteomics data reveal re-oxidation dynamics in the light, with the reduction and re-oxidation
791 network being linked to the Fdx-FTR and NTRC-2-Cys-Prx systems, respectively, while
792 plants use this redox network to fine-tune photosynthetic processes during the day.
793 Interestingly, such 2-Cys Prxs-mediated protein oxidation is also characterized in human cell
794 lines (Stöcker et al., 2018), indicating oxidative signal transduction to be ubiquitous among
795 different organisms.

796

797 **NTRC as well as *f*- and *m*-type Trxs play major roles to reduce the proteins of plastid**
798 **carbon metabolism with their individual impacts depending on the light conditions**

799 Our redox proteomics data show that in constant ML, almost all CBC enzymes and
800 proteins of related pathways displayed increased oxidation states in the *trxf1f2* and *ntrc*
801 mutants relative to wild type (Fig. 5D), reinforcing the notion that, both, *f*-type Trxs and
802 NTRC are involved in the redox-activation of CBC enzymes under normal light conditions *in*
803 *vivo*, although the effect of the latter was found to be indirect (Yoshida et al., 2015; Yoshida
804 and Hisabori, 2016; Guinea Diaz et al., 2020; Thormählen et al. 2015). In contrast to this, the
805 *trxm1m2* mutant showed only a minor impact on CBC protein oxidation states in ML, but a
806 stronger impact in FL, indicating *m*-type Trxs to be more important to regulate the redox
807 states of CBC enzymes in FL than in the ML environments (Fig. 5D). Indeed, several studies
808 proposed a specific importance of *m*-type Trxs, but not *f*-type Trxs, in photosynthetic
809 acclimation to FL and LL environments (Thormählen et al., 2017; Da et al., 2018; Okegawa
810 and Motohashi, 2020). In contrast to this, deficiency of NTRC strongly increased the
811 oxidation levels of CBC proteins and proteins of related pathways, both, in ML and FL (Fig.
812 5D). The wide oxidation effect of NTRC deficiency on plastidial targets is most likely
813 attributable to decreased provision of electrons to 2-Cys Prx leading to increased oxidation of
814 plastidial Trxs (Vaseghi et al., 2018; Cejudo et al., 2019). To sum up, these results indicate
815 plants to flexibly adopt different Trx systems to optimize redox regulation of plastidial targets
816 in acclimation to different light conditions.

817

818 **NTRC controls the oxidation levels of proteins of photosynthetic light reactions**

819 Our data show that deficiency in NTRC also affects the oxidation levels of proteins of
820 the photosynthetic machinery, which is more evident in FL than in ML, where PSI proteins
821 became more strongly reduced, while PSII proteins showed markedly increased oxidation
822 levels (Fig. 5, A and B). It has been proposed that deficiency of NTRC restricts the electron
823 donation to PSI (Naranjo et al., 2016b), but this seems to have minor effects on the oxidation
824 levels of PSI proteins in ML (Fig. 5A). In contrast, NTRC deficiency led to a marked
825 increase in reduction in PSI proteins in FL (Fig. 5A), which is most likely attributable to
826 decreased electron transfer from PSI to CBC due to an inhibition of the later. Indeed,
827 previous studies show that in FL, *ntrc* mutants display higher acceptor side limitation of PSI
828 (Y(NA)) than the wild type (Nikkanen et al., 2018). Subsequently, this over-reduction of PSI
829 will promote ROS generation, which may ultimately lead to increased oxidation of ROS-
830 sensitive PSII proteins (Fig. 5B). Collectively, the results suggest that NTRC is an important
831 hub in controlling the redox homeostasis of light reactions, especially in FL. This is in line
832 with *ntrc* mutants showing a decreased photosynthetic performance, specifically in FL
833 (Thormählen et al., 2017). In contrast, *trxf1f2* and *trxm1m2* mutants exhibited only mild and

834 inconsistent oxidation changes of photosystem proteins, compared to wild type (Fig. 5, A and
835 B). The relevance of the redox changes of photosystem proteins to determine the
836 photosynthetic performance of these mutants requires further investigations.

837

838 **NTRC/Trx systems regulate rapid changes in the oxidation state of proteins involved in** 839 **isoprenoid synthesis during alternating HL and LL phases of FL**

840 Our results show that the oxidation states of key enzymes of plastidial isoprenoid
841 synthesis, which have been suggested to be regulated by thiol/disulfide modulation in
842 previous studies, were strongly affected in *trxf1f2*, *trxm1m2* or *ntrc* mutants, depending on
843 the light conditions (Supplemental Fig. S3). There were specifically strong effects on VDE1.
844 In ML, the oxidation states of VDE1 in all three mutant lines were only slightly altered,
845 compared to wild type. This observation is in line with a previous study, showing that
846 deficiency of NTRC does not significantly affect VDE redox state in regular light conditions
847 (Naranjo et al., 2016b). This differs in plants growing in FL environments. Here VDE1 was
848 subject to a dramatic decrease in oxidation level in *trxm1m2* and *ntrc* mutants, specifically
849 during the HL phases of FL (1 min), while there was a marked increase in its oxidation status
850 during the subsequent LL phases (5 min; Supplemental Fig. S3). VDE proteins are the key
851 enzymes of the xanthophyll cycle, which is responsible for dissipating excess light energy
852 (Havaux et al., 2007; Fernández-Marín et al., 2021). An *in vitro* assay suggested that VDE
853 remains active only when it is completely oxidized (Yamamoto and Kamite, 1972; Simionato
854 et al., 2015). The de-epoxidation of violaxanthin is usually more active during HL as plants
855 need to dissipate excess light energy. In this context, the decreased VDE1 oxidation in *trxf1f2*,
856 *trxm1m2* and *ntrc* mutants suggests the interference of violaxanthin de-epoxidation in the HL
857 phases of FL. Collectively, the results indicate that the NTRC-Trx system operates to regulate
858 VDE1 redox states when plant experience FL.

859

860 **The influence of NTRC or Trxs *m1/m2* on the redox states of other chloroplast Trxs is** 861 **specifically strong during rapid fluctuations in light intensities**

862 Our redox proteomics data showed that 6-h into the photoperiod in ML, Trxs *f1/f2*,
863 Trxs *m1/m2* and NTRC deficiencies had only minor effects on the oxidation levels of other
864 pTrxs (Fig. 6B). Compared to this, the dysregulation of the redox balance in other pTrxs
865 became clearer in FL, specifically in *ntrc* and *trxm1m2* mutants, showing an increased
866 oxidation pattern in most of these proteins in the HL periods (Fig. 6B). This is in line with
867 previous studies showing increased oxidation states of Trxs *f1* and *f2* in the *ntrc* mutant,
868 compared to wild-type, as a short-term response during dark-light transitions (Pérez-Ruiz et

869 al., 2017). Accordingly, we hypothesize a role of NTRC and Trxs *m1/m2* to balance the redox
870 state of other types of Trxs to cope with short-term light fluctuations. This is in line with the
871 hypothesis suggesting NTRC to indirectly modulate the redox states of other pTrxs,
872 especially the *f*-type Trxs, via its role in balancing the 2-Cys Prx redox state (Cejudo et al.,
873 2019). Mechanistically speaking, the operation of NTRC substantially provides reducing
874 equivalents to 2-Cys Prxs and therefore minimizes the drainage of reducing equivalents from
875 the pools of other types of Trxs to 2-Cys Prxs (Vaseghi et al., 2018; Cejudo et al., 2019). Our
876 data indicate that in this context, the impact of NTRC is stronger during short-term
877 fluctuations in light intensity than in long-term constant light.

878

879 **Proteins of nitrogen and sulfur metabolism are linked to light-responsive redox** 880 **regulation via NTRC-Trx systems**

881 The marked changes in the oxidation states of GLU1 and GLT1 upon illumination led
882 us to assume that nitrogen metabolism is under the thiol-redox control in response to light
883 (Fig. 2G). It has been proposed in previous studies that the glutamine synthetase
884 (GS)/glutamate synthase (GOGAT) plays a central role in leaf nitrogen assimilation. GLU1
885 as the major GOGAT enzyme is predominately expressed in leaf tissues, and it accounts for
886 95% of the GOGAT activity (Somerville and Ogren, 1980; Coschigano et al., 1998; Coruzzi,
887 2003). GLU1 mainly uses the electrons from Fdx to catalyze glutamate synthesis (Suzuki and
888 Knaff, 2005). Its activity and protein accumulation are enhanced during the day (Coschigano
889 et al., 1998; Schjoerring et al., 2006). In fact, we detected less oxidized form of GLU1
890 protein upon illumination (Fig. 2G). In the context, the accumulating GLU1 proteins is
891 subject to a strong reduction during the day. This is in line with previous studies, showing
892 DTT treatment or addition of pTrxs to activate Fdx-dependent GOGAT isolated from spinach
893 chloroplasts (Lichter and Haberlein, 1998). The reduction of GLU1 may therefore lead to
894 increased activity of the GS/GOGAT cycle during the day. Interestingly, the NADH-
895 dependent GOGAT, GLT1, showed a marked oxidation pattern upon illumination. Such
896 oxidation may explain why GLT1 maintains in a very low level of leaf GOGAT activity
897 (Somerville and Ogren, 1980; Coschigano et al., 1998; Coruzzi, 2003). Our data also indicate
898 redox-control of aspartate synthesis. The oxidized level of ASP5 markedly decreased during
899 the day (Fig. 2G), indicating its strong reduction. However, this probably does not change
900 aspartate synthesis since previous studies analyzing a missense mutant of ASP5 shows that
901 interfering ASP5 activity does not change the levels of aspartate and asparagine (Miesak and
902 Coruzzi, 2002). Nevertheless, our results suggest ASP5 harbors redox-active Cys residues,
903 and its redox state is regulated by light. Furthermore, the oxidation levels of GLU1 and ASP5

904 moderately increased in mutants deficient in *f*-, *m*-type Trxs or NTRC, confirming their
905 regulation by the Trx/NTRC systems (Fig. 6D), which may explain changes in amino acid
906 accumulation (Thormählen et al., 2015).

907 Our data also show interesting changes in the oxidation states of proteins involved in
908 sulfur metabolism. Upon illumination, the oxidation levels of three ATP sulfurylase (ATPS)
909 proteins were significantly increased (Fig. 2G), which is in line with previous study showing
910 ATPS proteins to be targets of Trxs (Marchand et al., 2006). Fdx-dependent sulfite reductase
911 (SIR1), a further enzyme of S-assimilation which has been confirmed as Trx target in
912 previous studies (Lindahl and Kieselbach, 2009), showed increased oxidation levels in *trxf1f2*,
913 *trxm1m2* and *ntrc* mutants, compared to wild type (Fig. 6D). Taken together, our redox
914 proteomics data provide additional evidence that nitrogen and sulfur metabolism are
915 associated with NTRC/Trx-mediated redox regulation *in vivo*.

916

917 **Protein metabolism is subject to redox regulation via NTRC/Trx systems**

918 Our redox proteomics data show that a large set of proteins involved in different
919 processes of protein metabolism were subject to changes in their oxidation levels in response
920 to illumination (Fig. 1B and 4B), indicating redox regulation to be also operational in protein
921 homeostasis. This is in line with two recent articles suggesting thiol-based redox switches to
922 be operational at each step of translation and to play a major role in controlling protein
923 homeostasis (Moore et al., 2016; Topf et al., 2018). In the redoxome conducted in yeast, the
924 authors proposed that ribosomal proteins can serve as sensors to monitor cellular redox states
925 to modulate translation processes in response to environmental changes (Topf et al., 2018).
926 This suggests that the decrease in oxidation levels of plastidial ribosomal proteins during
927 dark-to-light transition may act as an additional “kick-off” signal to activate photosynthetic
928 processes. There is also evidence that the redox states of these plastidial ribosomal proteins
929 are under the control of the NTRC/Trx systems, since their oxidation levels were markedly
930 changed in mutants deficient in *f*-, *m*-type Trx or NTRC in ML (Supplemental Fig. S5).

931 The underlying mechanisms by which redox modifications of ribosomal proteins
932 modulate translational processes are still unclear. Interestingly, in our redox-proteomics study
933 we identified a well-known chloroplastic elongation factor (CPEFG), which was
934 characterized by markedly decreased oxidation levels upon illumination, while its oxidation
935 levels increased in *trxf1f2*, *trxm1m2* and *ntrc* mutants relative to wild type in either ML or FL
936 (Fig. 2H and Supplemental Fig. S5). This indicates the redox state of CPEFG to be controlled
937 by NTRC/Trx systems in response to light. In confirmation to this, the homologue of CPEFG
938 in the cyanobacterium *Synechocystis* was found to be subject to redox regulation by the NTR-

939 Trx system in previous studies. The reduced form of CPEFG can actively facilitate
940 translation processes (Kojima et al., 2009). Furthermore, deficiency of CPEFG in
941 Arabidopsis was found to strongly delay the accumulation of plastid proteins (LHCP, D1 and
942 CP22) including Rubisco subunits, resulting in an *albino* phenotype at early developmental
943 stages (Albrecht et al., 2006). Taken together, we propose that Trx/NTRC-dependent
944 reduction of CPEFG upon illumination will facilitate the translation of plastid-encoded
945 transcripts to optimize protein homeostasis inside the chloroplast.

946

947 **Conclusion remark**

948 In this study we used redox proteomics to systematically investigate the dynamics of
949 the thiol-redox network in plants in response to temporal changes in light availability and
950 across genotypes lacking different parts of NTRC/Trx systems. We found light to lead to
951 reduction and re-oxidation dynamics of photosynthetic proteins linked to the Fdx/Trx (*f*, *m*
952 and *x*-type Trxs) and the NTRC/2-Cys-Prx systems (including Trx *y2*), respectively, which
953 showed opposite changes in their light-responsive redox patterns. While deficiencies in *f*-type
954 Trxs, *m*-type Trxs or NTRC were mainly associated with increased oxidation states of
955 photosynthetic proteins, their impacts differed in different light environments, with NTRC
956 and Trxs *f1/f2* being important to keep proteins in a reduced state in constant light, while
957 NTRC and Trxs *m1/m2* being indispensable to balance oxidation/reduction-dynamics of
958 proteins during rapid alterations in light intensity in FL environments.

959

960

961 **Materials and Methods**

962 *Plant material and growth conditions*

963 The wild-type Arabidopsis plant, Columbia-0 (Col-0), and the well-characterized T-DNA
964 insertion mutant lines *trxf1f2* (SALK_128365/GK-020E05-013161; Naranjo et al., 2016a),
965 *trxm1m2* double mutants (SALK_123570/SALK_130686; Thormählen et al., 2017) and
966 *ntrc* single mutant (SALK_012208, Serrato et al., 2004), were used for the following analyses.
967 All plants were grown in a growth chamber equipped with LED light. The light intensity was
968 set as 150 $\mu\text{mol photons m}^{-2} \text{s}^{-1}$ with a 12-h-dark/12-h-light regime and the temperature was
969 set as 22°C. After three weeks, half of the plants were shifted to fluctuating light (FL) where
970 they were repeatedly exposed to 1 min high light (HL; 550 $\mu\text{mol photons m}^{-2} \text{s}^{-1}$) and 5 min
971 low light (LL; 50 $\mu\text{mol photons m}^{-2} \text{s}^{-1}$) in the same dark-to-light regime, while the other half
972 remained in the initial constant medium light (ML) conditions. The plants were then grown
973 for another week in the respective light conditions, before whole rosette leaves were sampled
974 six hours into the photoperiod by shock freezing in liquid nitrogen. In FL, leaf samples were
975 taken in HL and LL periods separately.

976

977 *RNA extraction, reverse transcription and real-time quantitative PCR*

978 The leaf material was frozen in liquid nitrogen and ground to fine powder. Approximate 50
979 mg of leaf powder was used for RNA extraction by implementing RNazol reagent (Sigma-
980 Aldrich). The RNA concentration was determined using NanoDrop spectrophotometer (ND-
981 2000, ThermoFisher Scientific), and 500 ng of total RNA was used to synthesize cDNA
982 using iScript reverse transcription kit (Biorad). The cDNA sample was diluted 20 times with
983 nuclease-free water, and 5 μL of diluted cDNA was implemented for real-time quantitative
984 PCR using the SYBG reagent (Biorad). The PCR reaction was performed in the thermocycler
985 (C1000 TouchTM Thermal Cycler; Biorad). The detailed protocol can be found in the
986 previous publication (Hou et al., 2021), and the primer pairs used in the real-time quantitative
987 PCR were listed below: TRXf1_qFW (5'-cgatgatctggttcagcg-3'), TRXf1_qRv (5'-
988 ctggtcatccggaagcag-3'), TRXf2_qFW (5'-tgtaaccaagacaacaagcca-3'), TRXf2_qRv (5'-
989 cggtcacttccttactacct-3'), TRXm1_qFW (5'-taacactgatgagtctcctgcaa-3'), TRXm1_qRv (5'-
990 gatgctggttgctaaagtgtctt-3'), TRXm2_qFW (5'-tgaagctcaggaaactactaccgat-3'), TRXm2_qRV
991 (5'-cagtgtaatgctgtgtagatcg-3'), NtrC_qFw (5'-tgaagatgaagaaagagtaccgag-3'), NtrC_qRv (5'-
992 ggtgtcctcattattggcct-3').

993

994 *Protein extraction and biotin-switch labeling method*

995 The biotin-switch assays were performed according to published methods with several
996 modifications (Jaffrey and Snyder, 2001; Liu et al., 2014). Briefly, 50 mg of finely pulverized
997 leaf sample was re-suspended in 350 μ L of extraction buffer (20 mM Tris-HCl, pH 7.0, 5
998 mM EDTA, 100 mM NaCl, 6M Urea) containing 50 mM NEM, and the whole extract was
999 incubated for 30 min at 25°C with mild shaking in the dark to alkylate free thiols. The leaf
1000 debris were removed by centrifugation at 20,000 x g for 10 min at 4°C, and the supernatant
1001 was mixed with 4 volumes of absolute acetone to precipitate protein. The protein pellet was
1002 recovered, cleaned up and dehydrated as mentioned above. The protein pellet was further re-
1003 suspended in 200 μ L of extraction buffer containing 100 mM dithiothreitol (DTT) followed
1004 by incubation for 30 min at 37°C with mild shaking in the dark to release oxidized thiols.
1005 Protein extract was subject to acetone precipitation, cleaned up and dehydrated as above. The
1006 protein pellet was re-suspended in 200 μ L of extraction buffer, and the protein concentration
1007 was determined using 660 nm protein reagent (Pierce). Approximate 80 μ g of total protein
1008 was used for biotin labeling in the presence of 0.4 mM thiol-reactive N-[6-(Biotinamido)
1009 hexyl]-3'-(2'-pyridyldithio) propionamide (biotin-HPDP; Cayman Chemical). The sample
1010 was then incubated for 60 min at 25°C with mild shaking in the dark followed by acetone
1011 precipitation and cleanup. The protein pellet was first re-suspended in 50 μ L of extraction
1012 buffer and further diluted by adding 450 μ L of binding buffer (20 mM Tris-HCl, pH 7.0; 5
1013 mM EDTA; 100 mM NaCl). The biotinylated protein extract was incubated with 100 μ L
1014 Streptavidin resin (Invitrogen) for 60 min at 25°C with mild shaking in the dark. The resin
1015 was recovered by centrifugation at 2000 xg for 1 min at 4°C. The protein-bound resin was
1016 washed three times with 500 μ L of binding buffer and twice with 500 μ L of 20 mM
1017 ammonium bicarbonate solution. The resin was incubated in 200 μ L of binding buffer
1018 containing 100 mM DTT for 30 min at 37°C with mild shaking in the dark to elute bound
1019 proteins. The eluted proteins were subject to acetone precipitation, cleaned up and dehydrated.

1020

1021 *Mass spectrometry*

1022 In Solution Tryptic Digest and LC-MS/MS Analysis was basically performed as described by
1023 (Hammel et al., 2018). Proteins were resuspended in 8M urea / ammonia bicarbonate buffer,
1024 digested using LysC and trypsin and desalted using home-made C18-STAGE tips. Finally,
1025 the peptides were resuspended in a solution of 2% acetonitrile, 2% formic acid. The LC-
1026 MS/MS system (Eksigent nanoLC 425 coupled to a TripleTOF 6600, ABSciex) was operated
1027 in μ -flow mode using a 25 μ -emitter needle in the ESI source. Peptides were separated by
1028 reversed phase (Triart C18, 5 μ m particles, 0.5 mm \times 5 mm as trapping column and Triart
1029 C18, 3 μ m particles, 300 μ m \times 150 mm as analytical column, YMC) using a flow rate of 4

1030 $\mu\text{l}/\text{min}$ and a gradient ramping from 1 to 5% HPLC buffer B (buffer A 2% acetonitrile, 0.1%
1031 formic acid; buffer B 90% acetonitrile, 0.1% formic acid) within 5 min, to 35% buffer B in
1032 73 min and to 50% buffer B in 2 min, followed by wash and equilibration steps. The mass
1033 spectrometer was operated in data-dependent analysis with one MS1 spectrum (350 to 1,250
1034 m/z, 250 ms) and 35 triggered MS/MS scans in high sensitivity mode (110 to 1,600 m/z, 50
1035 ms) for >2 times charged ions, resulting in a total cycle time of 2,050 ms. Fragmented
1036 precursors were excluded for 10 s and precursors with a response below 150 cps were
1037 excluded completely from MS/MS analysis.

1038

1039 *Mass spectrometry data analyses*

1040 Analysis of MS raw data was performed using MaxQuant version 1.6.0.1 using default
1041 settings with minor changes (Cox and Mann, 2008). Library generation for peptide spectrum
1042 matching was based on *Arabidopsis thaliana* (UniProt reference proteome UP0000065489)
1043 including chloroplast and mitochondrial proteins. Oxidation of methionine and acetylation of
1044 the N-termini were considered as peptide modifications. Maximal missed cleavages were set
1045 to 3 and peptide length to 6 amino acids, the maximal mass to 6,000 Da. Thresholds for
1046 peptide spectrum matching and protein identification were controlled for a false discovery
1047 rate (FDR) of 0.01. To account for the stochastic effect of data-dependent acquisition, match
1048 between runs (MBR) was used and to minimize the variation between different samples
1049 MaxQuant label-free quantification (LFQ) intensity values were reported. Raw data were
1050 deposited at PRIDE proteome exchange with identifier PXD043914. For further statistical
1051 analysis the identified proteins been detected in less than three biological replicates were
1052 considered as low-abundance targets, and omitted from the following data processing. The
1053 majority proteins IDs were used for the following annotation. The proteins IDs were
1054 converted to AGI locus codes using the online mapping tool provided by UniProt
1055 (<https://www.uniprot.org/id-mapping/>). The AGI locus codes were used to obtain gene names
1056 using the online tool, EnsemblPlants. The subcellular localizations of proteins were yielded
1057 from the SUBA4 database (Hooper et al., 2017). The biological functions of proteins were
1058 grouped using MapMan according to Araport and TAIR databases. The unsupervised cluster
1059 analyses were conducted using MapMan as well. The PCA was performed using the online
1060 tool, ClustVis (Metsalu and Vilo, 2015). The heatmaps, Venn diagrams and statistical
1061 analyses were performed using the R program. The other plots were graphed using the
1062 Graphpad Prism version 9.

1063

1064 *Validation of the results by an independent method*

1065 Redox proteomics results were validated by electrophoretic mobility shift assays as an
1066 independent method. The protein redox states of CFBPase, GAPDH and PRK were analyzed
1067 via protein electrophoretic mobility shift assay as described previously with several
1068 modifications (Muthuramalingam et al., 2010; Nikkanen et al., 2016). In brief, 20 mg of
1069 ground leaf powder was re-suspended in 200 μ L of 10% (w/v) Trichloroacetic acid solution
1070 followed by incubation on ice for 20 min. The supernatant was removed by centrifugation at
1071 20,000 \times g for 10 min at 4°C, and the protein pellet was washed twice with 1 mL of 80% (v/v)
1072 acetone prepared in 50 mM Tris-HCl (pH7.0). The protein pellet was dehydrated and then re-
1073 suspended in 200 μ L of extraction buffer (100 mM Tris-HCl, pH7.5, 1 mM EDTA, 2% [w/v]
1074 SDS, 6 M urea, proteinase inhibitor cocktail) containing 50 mM N-ethylmaleimide (NEM)
1075 followed by incubation for 30 min at 25°C with mild shaking in the dark to alkylate free
1076 thiols. The supernatant was recovered via centrifugation at 20,000 \times g for 5 min at 4°C. Equal
1077 amount of 20% (w/v) Trichloroacetic acid solution was applied into the protein extract, and
1078 the whole mixture was incubated on ice for 20 min. The protein pellet was recovered, cleaned
1079 up and dehydrated as mentioned above. The protein pellet was further re-suspended in 200
1080 μ L of extraction buffer containing 100 mM dithiothreitol (DTT) followed by incubation for
1081 30 min at 37°C with mild shaking in the dark to release oxidized thiols. Equal amount of 20%
1082 (w/v) Trichloroacetic acid solution was applied into the protein extract to stop the reaction,
1083 and the whole mixture was incubated on ice for 20 min. The protein pellet was recovered,
1084 cleaned up and dehydrated as mentioned above. The protein pellet was next re-suspended in
1085 100 μ L of extraction buffer containing 10 mM of methoxypolyethylene glycol maleimide
1086 (Mal-PEG, 5 kDa, Sigma-Aldrich_63187) followed by incubation for 60 min at 27°C with
1087 mild shaking in the dark to label the reduced thiols. Two microliter of 1 M DTT was applied
1088 to stop the reaction, and 500 μ L of absolute acetone was applied into the protein extract to
1089 precipitate protein and get rid of excess Mal-PEG. The protein pellet was recovered, cleaned
1090 up and dehydrated as mentioned above. The protein pellet was solubilized in 2-time-strength
1091 Laemmli buffer (Laemmli, 1970). The protein samples were analyzed by SDS-PAGE and
1092 Western blot. CFBP was detected using a commercial FBPase1 antibody (Agriseria;
1093 AS194319), while GAPB and PRK were detected using antibodies as described previously
1094 (Teh et al., 2023). Theoretically, the mass shift of the protein, in which a single reduced
1095 disulphide was labeled with Mal-PEG, is 10 kDa. Nevertheless, due to the hydration of PEG,
1096 the actual mass shift could become larger, up to 22 kDa (Makmura et al., 2001; Peled-Zehavi
1097 et al., 2010).

1098

1099 **Supplemental Data**

1100 **Supplemental Figure S1. The procedures of samples preparation and redox proteomics.**

1101 (A) Arabidopsis plants were grown under light intensity of $150 \mu\text{mol photons m}^{-2} \text{s}^{-1}$ with a
1102 12-h-dark/12-h-light regime for 4 weeks. To monitor a time-course in the light, whole rosette
1103 leaves were sampled by shock-freezing in liquid nitrogen at end of night (EN) and 10, 120
1104 and 360 min into the photoperiod. (B) The leaf samples were used for protein extraction in
1105 the presence of NEM to block the free thiol residues followed by DTT treatment to reduce
1106 the oxidized thiols. The released thiols were labeled with redox-active biotin, and the protein
1107 extract was subject to affinity purification using a streptavidin column. The bound proteins
1108 were eluted via incubating with DTT.

1109

1110 **Supplemental Figure S2. Validation of the redox proteomics results by analyzing**
1111 **oxidized and reduced forms of CBC enzymes using protein electrophoretic mobility**
1112 **shift assays as an independent method.**

1113 The protein oxidation percentages of chloroplastic fructose 1,6-bisphosphatase (CFBP), glyceraldehyde-3-phosphate dehydrogenase B (GAPB)
1114 and phosphoribulokinase (PRK) were analyzed via protein electrophoretic mobility shift
1115 assay as an independent method. For three independent biological replicates, the reduced
1116 thiols of proteins were alkylated using NEM, and the oxidized thiols of proteins were
1117 released by treating with DTT. The released thiols were further labeled with
1118 methoxypolyethylene glycol maleimide, which resulted in an increase of protein mass of the
1119 oxidized form that became distinguishable from the reduced form during gel electrophoresis.
1120 The oxidized and reduced forms of the proteins are indicated on the immunoblots. The
1121 immunosignals marked “ox” and “re” represent the oxidized and reduced forms of proteins,
1122 respectively, while those marked with asterisk represent the signals of non-specific binding.
1123 The scanned blots were used to calculate oxidation percentages of CFBP, GAPB and PRK
1124 shown in Figure 3.

1125

1126 **Supplemental Figure S3. Molecular characterization of *trxf1f2*, *trxm1m2* and *ntrc***
1127 **mutant lines.**

1128 The expression levels of *Trx f1, f2, m1, m2* and *Ntr C* were detected using real-
1129 time quantitative PCR with gene-specific primers. The gene expression was quantified using
1129 $2^{-\Delta\Delta\text{Ct}}$ method. The symbol “nd” indicates “not detected”

1130

1131 **Supplemental Figure S4. Protein oxidation changes in lipid, nucleotide and secondary**
1132 **metabolism across *trxf1f2*, *trxm1m2* and *ntrc* mutants in constant and fluctuating light.**

1133 Heatmaps summarize the \log_2 fold changes of protein oxidation levels in Arabidopsis *trxf1f2*,
1134 *trxm1m2* or *ntrc* mutants relative to the wild type (Col-0). The targets with yellow

1135 background are proposed to be redox-regulated proteins according to previous studies
1136 (Lindahl and Kieselbach, 2009). Proteins were allocated to different groups of biological
1137 functions including lipid, nucleotide and secondary metabolism. Plants were grown in the
1138 same conditions as indicated in the legend to Figure 4. Data are the means of three to six
1139 biological replicates. ML, medium light; FL, fluctuating light; HL, high-light phase of FL;
1140 LL, low-light phase of FL; red = increased oxidation, blue = decreased oxidation. Raw data
1141 and statistics, see Supplemental Table S4.

1142

1143 **Supplemental Figure S5. Protein oxidation changes in protein metabolism across *trxf1f2*,**
1144 ***trxm1m2* and *ntrc* mutants in constant and fluctuating light.** Heatmaps summarize the
1145 log₂ fold changes of protein oxidation levels in Arabidopsis *trxf1f2*, *trxm1m2* or *ntrc* mutants
1146 relative to the wild type (Col-0). The targets with yellow background are proposed to be
1147 redox-regulated proteins according to previous studies (Lindahl and Kieselbach, 2009).
1148 Proteins were allocated to different groups of biological functions including protein synthesis,
1149 modification and degradation. Plants were grown in the same conditions as indicated in the
1150 legend to Figure 4. Data are the means of three to six biological replicates. ML, medium light;
1151 FL, fluctuating light; HL, high-light phase of FL; LL, low-light phase of FL; red = increased
1152 oxidation, blue = decreased oxidation. Raw data and statistics, see Supplemental Table S4.

1153

1154 **Supplemental Table S1.** Proteins showing statistically significant changes in oxidation states
1155 in response to illumination compared to the dark.

1156

1157 **Supplemental Table S2.** Proteins with light-dependent changes in oxidation levels that have
1158 been reported to be also subject to diurnal changes with respect to protein abundance. By
1159 comparing the list of proteins identified to be subject to light-dependent changes in oxidation
1160 levels in Supplemental Table S1 with the published data set of Uhrig et al. (2021), we found
1161 that only 16 out of 319 proteins were also reported to be subject to diurnal changes in overall
1162 protein levels.

1163

1164 **Supplemental Table S3.** Proteins displaying significant redox changes in all three time
1165 points of the photoperiod compared to the dark.

1166

1167 **Supplemental Table S4.** Proteins showing significant redox changes in Arabidopsis *trxf1f2*,
1168 *trxm1m2* or *ntrc* mutants with respect to the wild type (Col-0) during ML and FL.

1169

1170 **Supplemental Table S5.** Comparison of our present data set (Supplemental Table S4) with
1171 those of Dziubek et al., (2023) in ML and FL pinpoints 49 of the proteins that are relevant to
1172 our analyses and shown in Figures 5, 6, S4 and S5 to reveal significant changes in protein
1173 abundance. These proteins showed only very minor changes in their quantified levels (less
1174 than 3%) when mutants were compared to the wild type (Col-0), indicating that changes in
1175 protein expression levels can be neglected as possible errors in our study.

1176 **Funding:**

1177

1178 This work was supported by the Deutsche Forschungsgemeinschaft (TRR175).

1179

1180 **Acknowledgements**

1181 We are grateful to all green house staff at Faculty of Biology in Ludwig-Maximilians-
1182 University Munich for taking care of Arabidopsis plants.

1183

1184 **Figure legends**

1185 **Figure 1. Light-dependent dynamics in the landscape of protein-oxidation changes at**
1186 **different time points into the photoperiod.** Redox proteomics analyses of Arabidopsis
1187 plants sampled 10 (L10), 120 (L120) and 360 min (L360) into the photoperiod, compared to
1188 end of the night (EN, dark conditions). **(A)** Subcellular localization of proteins showing
1189 significant changes in their oxidation levels in the light, compared to the dark. **(B)** Functional
1190 categories of proteins showing significant changes in their oxidation levels in the light,
1191 compared to the dark. **(C)** Principal component analysis displaying the distinctions of protein
1192 oxidation states between EN, and L10, L120 and L360. **(D)** Venn diagram highlighting the
1193 distribution of proteins subject to significant changes in oxidation states at different time
1194 points into the photoperiod, compared to EN. **(E) - (H)** Unsupervised cluster analysis
1195 showing the grouping of proteins that display different redox changes in response to a time
1196 course in the light. **(I)** The subcellular localization of proteins from the different clusters. **(J)**
1197 The biological function categories of proteins from the different clusters. Data are based on
1198 three to six biological replicates.

1199

1200 **Figure 2. Protein-oxidation changes in photosynthetic processes, redox balance,**
1201 **metabolic pathways and protein metabolism in response to light.** The heatmaps
1202 summarize the log₂ fold changes of protein oxidation levels at 10 (L10), 120 (L120) and 360
1203 min (L360) into the photoperiod, relative to the end of the night (EN, dark conditions).
1204 Proteins were allocated to different groups of biological functions including **(A)** light reaction,
1205 **(B)** Calvin Benson Cycle (CBC), **(C)** major carbohydrate (CHO) metabolism, **(D)**
1206 thioredoxin, **(E)** redox homeostasis, **(F)** photorespiration (PR), **(G)** nitrogen and sulfur
1207 metabolism (N/S) and **(H)** protein metabolism. The protein metabolism group is further
1208 divided in to three subgroups including synthesis, modification and degradation (from up to
1209 down). Data are the means of three to six biological replicates. The proteins high-lighted with
1210 pink background are validated Trx targets, while those with yellow background have been
1211 proposed to be redox-regulated proteins according to previous studies (Lindahl and
1212 Kieselbach, 2009). red = increased oxidation, blue = decreased oxidation. Raw data and
1213 statistics, see Supplemental Table S1.

1214

1215 **Figure 3. Validation of the redox proteomics results by analyzing oxidation percentages**
1216 **of CBC enzymes using protein electrophoretic mobility shift assays as an independent**
1217 **method.** The protein oxidation percentages of chloroplastic fructose 1,6-bisphosphatase
1218 (CFBP), glyceraldehyde-3-phosphate dehydrogenase B (GAPB) and phosphoribulokinase

1219 (PRK) were analyzed via protein electrophoretic mobility shift assay as an independent
1220 method. For three independent biological replicates, the reduced thiols of proteins were
1221 alkylated using NEM, and the oxidized thiols of proteins were released by treating with DTT.
1222 The released thiols were further labeled with methoxypolyethylene glycol maleimide, which
1223 resulted in an increase of protein mass of the oxidized form that became distinguishable from
1224 the reduced form during gel electrophoresis. The oxidation percentages of CFBP, GAPB and
1225 PRK were calculated from the scanned blots shown in Supplemental Figure S2 by dividing
1226 the intensities of the bands reflecting the oxidized form by the sum of the intensities of the
1227 bands reflecting oxidized plus reduced forms of the respective protein. Results are means +/-
1228 SE ($n=3$). The symbol “nd” indicates “not detectable”.

1229

1230 **Figure 4. Dynamics in the landscape of protein oxidation changes across mutants**
1231 **lacking different parts of NTRC/Trx systems in constant and fluctuating light.** Redox
1232 proteomics analyses of Arabidopsis *trxf1f2*, *trxm1m2* or *ntrc* mutants relative to the wild type
1233 (Col-0). Plants were grown in the same conditions as in Figures 1-3 (ML = medium light) or
1234 in fluctuating light (FL) with rapidly alternating high light (HL, 1 min) and low light (LL, 5
1235 min) phases. Samples were taken 360 min into the photoperiod. (A) The subcellular
1236 localization of proteins showing significantly different oxidation states in the mutants relative
1237 to the wild type. (B) The functional categories of proteins showing significantly different
1238 oxidation states in the mutants relative to the wild type. (C) - (E) The principal component
1239 analysis displaying the distinctions of protein oxidation states between wild type (Col-0),
1240 *trxf1f2*, *trxm1m2* and *ntrc* mutants in ML or in HL or LL phases of FL. (F) - (H) Venn
1241 diagram highlighting the distribution of proteins subject to marked changes in their oxidation
1242 states in the respective mutants, compared to the wild type, during constant ML, as well as
1243 during HL or LL phases of FL. Data are based on three to six biological replicates.

1244

1245 **Figure 5. Protein oxidation changes in photosynthetic processes and carbohydrate**
1246 **metabolism across *trxf1f2*, *trxm1m2* and *ntrc* mutants in constant and fluctuating light.**
1247 Heatmaps summarize the log₂ fold changes of protein oxidation levels in Arabidopsis *trxf1f2*,
1248 *trxm1m2* or *ntrc* mutants relative to the wild type (Col-0). The proteins high-lighted with pink
1249 background are validated Trx targets, while those with yellow background have been
1250 proposed to be redox-regulated proteins according to previous studies (Lindahl and
1251 Kieselbach, 2009). Proteins were allocated to different groups of biological functions
1252 including (A) photosystem I (PSI), (B) photosystem II (PSII), (C) electron carrier and ATP
1253 synthase, (D) Calvin-Benson Cycle (CBC), (E) major carbohydrate (CHO) metabolism and

1254 (F) Tetrapyrrole. Plants were grown in the same conditions as indicated in the legend of
1255 Figure 4. Data are the means of three to six biological replicates. ML, medium light; FL,
1256 fluctuating light; HL, high-light phase of FL; LL, low-light phase of FL; red = increased
1257 oxidation, blue = decreased oxidation. Raw data and statistics, see Supplemental Table S4.

1258

1259 **Figure 6. Protein oxidation changes in redox homeostasis, photorespiration and amino**
1260 **acid metabolism across *trxf1f2*, *trxm1m2* and *ntrc* mutants in constant and fluctuating**
1261 **light.** Heatmaps summarize the log₂ fold changes of protein oxidation levels in Arabidopsis
1262 *trxf1f2*, *trxm1m2* or *ntrc* mutants relative to the wild type (Col-0). The proteins high-lighted
1263 with pink background are validated Trx targets, while those with yellow background have
1264 been proposed to be redox-regulated proteins according to previous studies (Lindahl and
1265 Kieselbach, 2009). Proteins were allocated to different groups of biological functions
1266 including (A) redox homeostasis, (B) thioredoxin (C) photorespiration (PR) and (D) nitrogen
1267 and sulfur metabolism (N/S). Plants were grown in the same conditions as indicated in the
1268 legend to Figure 4. Data are the means of three to six biological replicates. ML, medium light;
1269 FL, fluctuating light; HL, high-light phase of FL; LL, low-light phase of FL; red = increased
1270 oxidation, blue = decreased oxidation. Raw data and statistics, see Supplemental Table S4.

1271

1272 **Literature cited**

- 1273 **Albrecht V, Ingenfeld A, Apel K** (2006) Characterization of the snowy cotyledon 1
1274 mutant of *Arabidopsis thaliana*: The impact of chloroplast elongation factor G on
1275 chloroplast development and plant vitality. *Plant Mol Biol* **60**: 507–518
- 1276 **Alkhalfioui F, Renard M, Montrichard F** (2007) Unique properties of NADP-
1277 thioredoxin reductase C in legumes. *J Exp Bot.* doi: 10.1093/jxb/erl248
- 1278 **Arsova B, Hoja U, Wimmelbacher M, Greiner E, Üstün Ş, Melzer M, Petersen K, Lein
1279 W, Börnke F** (2010) Plastidial thioredoxin z interacts with two fructokinase-like
1280 proteins in a thiol-dependent manner: Evidence for an essential role in chloroplast
1281 development in *Arabidopsis* and *Nicotiana benthamiana*. *Plant Cell* **22**: 1498–1515
- 1282 **Balmer Y, Koller A, Del Val G, Manieri W, Schürmann P, Buchanan BB** (2003)
1283 Proteomics gives insight into the regulatory function of chloroplast thioredoxins.
1284 *Proc Natl Acad Sci U S A* **100**: 370–375
- 1285 **Balmer Y, Vensel WH, Hurkman WJ, Buchanan BB** (2006) Thioredoxin Target
1286 Proteins in Chloroplast Thylakoid Membranes. *Antioxid Redox Signal* **8**: 1829–
1287 1834
- 1288 **Balmer Y, Vensel WH, Tanaka CK, Hurkman WJ, Gelhaye E, Rouhier N, Jacquot JP,
1289 Manieri W, Schürmann P, Droux M, et al** (2004a) Thioredoxin links redox to the
1290 regulation of fundamental processes of plant mitochondria. *Proc Natl Acad Sci U S
1291 A* **101**: 2642–2647
- 1292 **Balmer Y, Vensel WH, Tanaka CK, Hurkman WJ, Gelhaye E, Rouhier N, Jacquot J-P,
1293 Manieri W, Schurmann P, Droux M, et al** (2004b) Thioredoxin links redox to the
1294 regulation of fundamental processes of plant mitochondria. *Proceedings of the
1295 National Academy of Sciences* **101**: 2642–2647
- 1296 **Bartsch S, Monnet J, Selbach K, Quigley F, Gray J, Von Wettstein D, Reinbothe S,
1297 Reinbothe C** (2008) Three thioredoxin targets in the inner envelope membrane of
1298 chloroplasts function in protein import and chlorophyll metabolism. *Proc Natl Acad
1299 Sci U S A* **105**: 4933–4938
- 1300 **Bashandy T, Taconnat L, Renou JP, Meyer Y, Reichheld JP** (2009) Accumulation of
1301 flavonoids in an ntra ntrb mutant leads to tolerance to UV-C. *Mol Plant* **2**: 249–258
- 1302 **Bohrer AS, Massot V, Innocenti G, Reichheld JP, Issakidis-Bourguet E, Vanacker H
1303** (2012) New insights into the reduction systems of plastidial thioredoxins point out
1304 the unique properties of thioredoxin z from *Arabidopsis*. *J Exp Bot* **63**: 6315–6323
- 1305 **Brandes HK, Larimer FW, Geck MK, Stringer CD, Schurmann P, Hartman FC** (1993)
1306 Direct identification of the primary nucleophile of thioredoxin f. *Journal of
1307 Biological Chemistry* **268**: 18411–18414
- 1308 **Carrillo LR, Froehlich JE, Cruz JA, Savage LJ, Kramer DM** (2016) Multi-level
1309 regulation of the chloroplast ATP synthase: The chloroplast NADPH thioredoxin
1310 reductase C (NTRC) is required for redox modulation specifically under low
1311 irradiance. *The Plant Journal* **87**: 654–663
- 1312 **Cejudo FJ, Ferrández J, Cano B, Puerto-Galán L, Guinea M** (2012) The function of the
1313 NADPH thioredoxin reductase C-2-Cys peroxiredoxin system in plastid redox
1314 regulation and signalling. *FEBS Lett* **586**: 2974–2980
- 1315 **Cejudo FJ, González MC, Pérez-Ruiz JM** (2021) Redox regulation of chloroplast
1316 metabolism. *Plant Physiol* **186**: 9–21
- 1317 **Cejudo FJ, Ojeda V, Delgado-Requerrey V, González M, Pérez-Ruiz JM** (2019)
1318 Chloroplast redox regulatory mechanisms in plant adaptation to light and darkness.
1319 *Front Plant Sci* **10**: 1–11
- 1320 **Cha JY, Kim JY, Jung IJ, Kim MR, Melencion A, Alam SS, Yun DJ, Lee SY, Kim MG, Kim
1321 WY** (2014) NADPH-dependent thioredoxin reductase A (NTRA) confers elevated

- 1322 tolerance to oxidative stress and drought. *Plant Physiology and Biochemistry* **80**:
1323 184–191
- 1324 **Chen Q, Xiao Y, Ming Y, Peng R, Hu J, Wang H, Jin H** (2022) Quantitative proteomics
1325 reveals redox-based functional regulation of photosynthesis under fluctuating light
1326 in plants. *J Integr Plant Biol* **64**: 2168–2186
- 1327 **Collin V, Issakidis-Bourguet E, Marchand C, Hirasawa M, Lancelin JM, Knaff DB,**
1328 **Miginiac-Maslow M** (2003) The Arabidopsis plastidial thioredoxins. New
1329 functions and new insights into specificity. *Journal of Biological Chemistry* **278**:
1330 23747–23752
- 1331 **Collin V, Lamkemeyer P, Miginiac-Maslow M, Hirasawa M, Knaff DB, Dietz KJ,**
1332 **Issakidis-Bourguet E** (2004) Characterization of plastidial thioredoxins from
1333 arabidopsis belonging to the new γ -type. *Plant Physiol* **136**: 4088–4095
- 1334 **Coruzzi GM** (2003) Primary N-assimilation into Amino Acids in Arabidopsis.
1335 *Arabidopsis Book* **2**: e0010
- 1336 **Coschigano KT, Melo-Oliveira R, Lim J, Coruzzi GM** (1998) Arabidopsis *gls* mutants
1337 and distinct Fd-GOGAT genes: Implications for photorespiration and primary
1338 nitrogen assimilation. *Plant Cell* **10**: 741–752
- 1339 **Cox J, Mann M** (2008) MaxQuant enables high peptide identification rates,
1340 individualized p.p.b.-range mass accuracies and proteome-wide protein
1341 quantification. *Nat Biotechnol* **26**: 1367–1372
- 1342 **Cremers CM, Jakob U** (2013) Oxidant sensing by reversible disulfide bond formation.
1343 *Journal of Biological Chemistry* **288**: 26489–26496
- 1344 **Da Q, Sun T, Wang M, Jin H, Li M, Feng D, Wang J, Wang H Bin, Liu B** (2018) M-type
1345 thioredoxins are involved in the xanthophyll cycle and proton motive force to alter
1346 NPQ under low-light conditions in Arabidopsis. *Plant Cell Rep* **37**: 279–291
- 1347 **Da Q, Wang P, Wang M, Sun T, Jin H, Liu B, Wang J, Grimm B, Wang H-B** (2017)
1348 Thioredoxin and NADPH-dependent thioredoxin reductase C regulation of
1349 Tetrapyrrole Biosynthesis. *Plant Physiol* **175**: 652–666
- 1350 **Delgado-Requerey V, Cejudo FJ, González M-C** (2023) The Functional Relationship
1351 between NADPH Thioredoxin Reductase C, 2-Cys Peroxiredoxins, and m-Type
1352 Thioredoxins in the Regulation of Calvin–Benson Cycle and Malate-Valve Enzymes
1353 in Arabidopsis. *Antioxidants* **12**: 1041
- 1354 **Dietz KJ, Hell R** (2015) Thiol switches in redox regulation of chloroplasts: Balancing
1355 redox state, metabolism and oxidative stress. *Biol Chem* **396**: 483–494
- 1356 **Dziubek D, Poeker L, Siemiątkowska B, Graf A, Marino G, Alseekh S, Arrivault S,**
1357 **Fernie AR, Armbruster U, Geigenberger P** (2023) NTRC and thioredoxins *m 1/ m*
1358 *2* underpin the light acclimation of plants on proteome and metabolome levels.
1359 *Plant Physiol*. doi: 10.1093/plphys/kiad535
- 1360 **Fernández-Marín B, Roach T, Verhoeven A, García-Plazaola JI** (2021) Shedding light
1361 on the dark side of xanthophyll cycles. *New Phytologist* **230**: 1336–1344
- 1362 **Geigenberger P, Thormählen I, Daloso DM, Fernie AR** (2017) The Unprecedented
1363 Versatility of the Plant Thioredoxin System. *Trends Plant Sci* **22**: 249–262
- 1364 **Goyer A, Haslekås C, Miginiac-Maslow M, Klein U, Le Marechal P, Jacquot JP,**
1365 **Decottignies P** (2002) Isolation and characterization of a thioredoxin-dependent
1366 peroxidase from *Chlamydomonas reinhardtii*. *Eur J Biochem* **269**: 272–282
- 1367 **Guinea Diaz M, Nikkanen L, Himanen K, Toivola J, Rintamäki E** (2020) Two
1368 chloroplast thioredoxin systems differentially modulate photosynthesis in
1369 Arabidopsis depending on light intensity and leaf age. *Plant Journal* **104**: 718–734
- 1370 **Hall M, Mata-Cabana A, Åkerlund HE, Florencio FJ, Schröder WP, Lindahl M,**
1371 **Kieselbach T** (2010) Thioredoxin targets of the plant chloroplast lumen and their
1372 implications for plastid function. *Proteomics* **10**: 987–1001

- 1373 **Hammel A, Zimmer D, Sommer F, Mühlhaus T, Schroda M** (2018) Absolute
1374 Quantification of Major Photosynthetic Protein Complexes in *Chlamydomonas*
1375 *reinhardtii* Using Quantification Concatamers (QconCATs). *Front Plant Sci.* doi:
1376 10.3389/fpls.2018.01265
- 1377 **Hanke GT, Okutani S, Satomi Y, Takao T, Suzuki A, Hase T** (2005) Multiple iso-
1378 proteins of FNR in *Arabidopsis*: Evidence for different contributions to chloroplast
1379 function and nitrogen assimilation. *Plant Cell Environ* **28**: 1146–1157
- 1380 **Havaux M, Dall’Osto L, Bassi R** (2007) Zeaxanthin Has Enhanced Antioxidant Capacity
1381 with Respect to All Other Xanthophylls in *Arabidopsis* Leaves and Functions
1382 Independent of Binding to PSII Antennae. *Plant Physiol* **145**: 1506–1520
- 1383 **Heber UW, Santarius KA** (1965) Compartmentation and reduction of pyridine
1384 nucleotides in relation to photosynthesis. *Biochim Biophys Acta* **109**: 390–408
- 1385 **Hieber AD, Bugos RC, Yamamoto HY** (2000) Plant lipocalins: violaxanthin de-
1386 epoxidase and zeaxanthin epoxidase. *Biochimica et Biophysica Acta (BBA) - Protein*
1387 *Structure and Molecular Enzymology* **1482**: 84–91
- 1388 **Holmgren A** (1995) Thioredoxin structure and mechanism: conformational changes on
1389 oxidation of the active-site sulfhydryls to a disulfide. *Structure* **3**: 239–243
- 1390 **Hooper CM, Castleden IR, Tanz SK, Aryamanesh N, Millar AH** (2017) SUBA4: the
1391 interactive data analysis centre for *Arabidopsis* subcellular protein locations.
1392 *Nucleic Acids Res* **45**: D1064–D1074
- 1393 **Hou LY, Lehmann M, Geigenberger P** (2021) Thioredoxin h2 and o1 show different
1394 subcellular localizations and redox-active functions, and are extrachloroplastic
1395 factors influencing photosynthetic performance in fluctuating light. *Antioxidants.*
1396 doi: 10.3390/antiox10050705
- 1397 **Jacquot JP, Eklund H, Rouhier N, Schürmann P** (2009) Structural and evolutionary
1398 aspects of thioredoxin reductases in photosynthetic organisms. *Trends Plant Sci* **14**:
1399 336–343
- 1400 **Jaffrey SR, Snyder SH** (2001) The Biotin Switch Method for the Detection of S -
1401 Nitrosylated Proteins. *Science’s STKE.* doi: 10.1126/stke.2001.86.pl1
- 1402 **Jurado-Flores A, Delgado-Requerey V, Gálvez-Ramírez A, Puerto-Galán L, Pérez-**
1403 **Ruiz JM, Cejudo FJ** (2020) Exploring the functional relationship between ytype
1404 thioredoxins and 2-cys peroxiredoxins in *arabidopsis* chloroplasts. *Antioxidants* **9**:
1405 1–18
- 1406 **Kang Z, Qin T, Zhao Z** (2019) Thioredoxins and thioredoxin reductase in chloroplasts:
1407 A review. *Gene* **706**: 32–42
- 1408 **Kirchsteiger K, Pulido P, Gonzálezlez M, Cejudo FJ** (2009) NADPH Thioredoxin
1409 reductase C controls the redox status of chloroplast 2-Cys peroxiredoxins in
1410 *arabidopsis thaliana*. *Mol Plant* **2**: 298–307
- 1411 **Kojima K, Motohashi K, Morota T, Oshita M, Hisabori T, Hayashi H, Nishiyama Y**
1412 (2009) Regulation of translation by the Redox State of Elongation factor G in the
1413 cyanobacterium *Synechocystis* sp. PCC 6803. *Journal of Biological Chemistry* **284**:
1414 18685–18691
- 1415 **Laemmli UK** (1970) Cleavage of structural proteins during the assembly of the head of
1416 bacteriophage T4. *Nature* **227**: 680–685
- 1417 **Lamkemeyer P, Laxa M, Collin V, Li W, Finkemeier I, Schöttler MA, Holtkamp V,**
1418 **Tognetti VB, Issakidis-Bourguet E, Kandlbinder A, et al** (2006) Peroxiredoxin Q
1419 of *Arabidopsis thaliana* is attached to the thylakoids and functions in context of
1420 photosynthesis. *Plant Journal* **45**: 968–981
- 1421 **Lampl N, Lev R, Nissan I, Gilad G, Hipsch M, Rosenwasser S** (2022) Systematic
1422 monitoring of 2-Cys peroxiredoxin-derived redox signals unveiled its role in
1423 attenuating carbon assimilation rate. *Proc Natl Acad Sci U S A* **119**: 1–10

- 1424 **Lemaire SD, Guillont B, Le Maréchal P, Keryer E, Miginiac-Maslow M, Decottignies**
1425 **P** (2004) New thioredoxin targets in the unicellular photosynthetic eukaryote
1426 *Chlamydomonas reinhardtii*. *Proc Natl Acad Sci U S A* **101**: 7475–7480
- 1427 **Lepistö A, Pakula E, Toivola J, Krieger-Liszkay A, Vignols F, Rintamäki E** (2013)
1428 Deletion of chloroplast NADPH-dependent thioredoxin reductase results in
1429 inability to regulate starch synthesis and causes stunted growth under short-day
1430 photoperiods. *J Exp Bot* **64**: 3843–3854
- 1431 **Lichter A, Haberlein I** (1998) A light-dependent redox signal participates in the
1432 regulation of ammonia fixation in chloroplasts of higher plants - Ferredoxin:
1433 Glutamate synthase is a thioredoxin-dependent enzyme. *J Plant Physiol* **153**: 83–90
- 1434 **Lindahl M, Florencio FJ** (2003) Thioredoxin-linked processes in cyanobacteria are as
1435 numerous as in chloroplasts, but targets are different. *Proc Natl Acad Sci U S A* **100**:
1436 16107–16112
- 1437 **Lindahl M, Kieselbach T** (2009) Disulphide proteomes and interactions with
1438 thioredoxin on the track towards understanding redox regulation in chloroplasts
1439 and cyanobacteria. *J Proteomics* **72**: 416–438
- 1440 **Liu P, Zhang H, Wang H, Xia Y** (2014) Identification of redox-sensitive cysteines in the
1441 arabidopsis proteome using OxiTRAQ, a quantitative redox proteomics method.
1442 *Proteomics* **14**: 750–762
- 1443 **Löwe O, Rezende F, Heidler J, Wittig I, Helfinger V, Brandes RP, Schröder K** (2019)
1444 BIAM switch assay coupled to mass spectrometry identifies novel redox targets of
1445 NADPH oxidase 4. *Redox Biol* **21**: 101125
- 1446 **Makmura L, Hamann M, Areopagita A, Furuta S, Muñoz A, Momand J** (2001)
1447 Development of a Sensitive Assay to Detect Reversibly Oxidized Protein Cysteine
1448 Sulfhydryl Groups. *Antioxid Redox Signal* **3**: 1105–1118
- 1449 **Marchand C, Le Maréchal P, Meyer Y, Decottignies P** (2006) Comparative proteomic
1450 approaches for the isolation of proteins interacting with thioredoxin. *Proteomics* **6**:
1451 6528–6537
- 1452 **Marchand CH, Vanacker H, Collin V, Issakidis-Bourguet E, Le Maréchal P,**
1453 **Decottignies P** (2010) Thioredoxin targets in Arabidopsis roots. *Proteomics* **10**:
1454 2418–2428
- 1455 **McFarlane CR, Shah NR, Kabasakal B V., Echeverria B, Cotton CAR, Bubeck D,**
1456 **Murray JW** (2019) Structural basis of light-induced redox regulation in the Calvin–
1457 Benson cycle in cyanobacteria. *Proceedings of the National Academy of Sciences*
1458 **116**: 20984–20990
- 1459 **Metsalu T, Vilo J** (2015) ClustVis: a web tool for visualizing clustering of multivariate
1460 data using Principal Component Analysis and heatmap. *Nucleic Acids Res* **43**:
1461 W566–W570
- 1462 **Meyer Y, Belin C, Delorme-Hinoux V, Reichheld J-P, Riondet C** (2012) Thioredoxin
1463 and glutaredoxin systems in plants: Molecular mechanisms, crosstalks, and
1464 functional significance. *Antioxid Redox Signal* **17**: 1124–1160
- 1465 **Michalska J, Zauber H, Buchanan BB, Cejudo FJ, Geigenberger P** (2009) NTRC links
1466 built-in thioredoxin to light and sucrose in regulating starch synthesis in
1467 chloroplasts and amyloplasts. *Proceedings of the National Academy of Sciences*
1468 **106**: 9908–9913
- 1469 **Michelet L, Lemaire SD, Marchand CH, Fermani S, Sparla F, Morisse S, Pérez-Pérez**
1470 **ME, Trost P, Zaffagnini M, Danon A, et al** (2013) Redox regulation of the Calvin–
1471 Benson cycle: something old, something new. *Front Plant Sci* **4**: 1–21
- 1472 **Miesak BH, Coruzzi GM** (2002) Molecular and physiological analysis of Arabidopsis
1473 mutants defective in cytosolic or chloroplastic aspartate aminotransferase. *Plant*
1474 *Physiol* **129**: 650–660

- 1475 **Montrichard F, Alkhalifioui F, Yano H, Vensel WH, Hurkman WJ, Buchanan BB**
1476 (2009) Thioredoxin targets in plants: The first 30 years. *J Proteomics* **72**: 452–474
- 1477 **Moore M, Gossmann N, Dietz KJ** (2016) Redox Regulation of Cytosolic Translation in
1478 Plants. *Trends Plant Sci* **21**: 388–397
- 1479 **Muthuramalingam M, Dietz K-J, Ströher E** (2010) Thiol–Disulfide Redox Proteomics
1480 in Plant Research. *NIH Public Access* **639**: 1–14
- 1481 **Naranjo B, Diaz-Espejo A, Lindahl M, Cejudo FJ** (2016a) Type-f thioredoxins have a
1482 role in the short-term activation of carbon metabolism and their loss affects growth
1483 under short-day conditions in *Arabidopsis thaliana*. *J Exp Bot* **67**: 1951–1964
- 1484 **Naranjo B, Migné C, Krieger-Liszkay A, Hornero-Méndez D, Gallardo-Guerrero L,**
1485 **Cejudo FJ, Lindahl M** (2016b) The chloroplast NADPH thioredoxin reductase C,
1486 NTRC, controls non-photochemical quenching of light energy and photosynthetic
1487 electron transport in *Arabidopsis*. *Plant Cell Environ* **39**: 804–822
- 1488 **Navrot N, Collin V, Gualberto J, Gelhaye E, Hirasawa M, Rey P, Knaff DB, Issakidis E,**
1489 **Jacquot JP, Rouhier N** (2006) Plant glutathione peroxidases are functional
1490 peroxiredoxins distributed in several subcellular compartments and regulated
1491 during biotic and abiotic stresses. *Plant Physiol* **142**: 1364–1379
- 1492 **Niedermaier S, Schneider T, Bahl MO, Matsubara S, Huesgen PF** (2020)
1493 Photoprotective Acclimation of the *Arabidopsis thaliana* Leaf Proteome to
1494 Fluctuating Light. *Front Genet* **11**: 1–15
- 1495 **Nikkanen L, Toivola J, Rintamäki E** (2016) Crosstalk between chloroplast thioredoxin
1496 systems in regulation of photosynthesis. *Plant Cell Environ* **39**: 1691–1705
- 1497 **Nikkanen L, Toivola J, Trotta A, Manuel J, Diaz G, Tikkanen M, Aro E-M, Rintamäki**
1498 **E** (2018) Regulation of cyclic electron flow by chloroplast NADPH-dependent
1499 thioredoxin system. doi: 10.1101/261560
- 1500 **Ojeda V, Pérez-Ruiz JM, González M, Nájera VA, Sahrawy M, Serrato AJ,**
1501 **Geigenberger P, Cejudo FJ** (2017) NADPH Thioredoxin Reductase C and
1502 Thioredoxins Act Concertedly in Seedling Development. *Plant Physiol* **174**: 1436–
1503 1448
- 1504 **Okegawa Y, Motohashi K** (2015) Chloroplastic thioredoxin m functions as a major
1505 regulator of Calvin cycle enzymes during photosynthesis in vivo. *Plant Journal* **84**:
1506 900–913
- 1507 **Okegawa Y, Motohashi K** (2020) M-type thioredoxins regulate the PGR5/PGRL1-
1508 dependent pathway by forming a disulfide-linked complex with PGRL1. *Plant Cell*
1509 **32**: 3866–3883
- 1510 **Parker J, Balmant K, Zhu F, Zhu N, Chen S** (2015) CysTMTRAQ - An integrative
1511 method for unbiased thiol-based redox proteomics. *Molecular and Cellular*
1512 *Proteomics* **14**: 237–242
- 1513 **Peled-Zehavi H, Avital S, Danon A** (2010) Methods of redox signaling by plant
1514 thioredoxins. *Methods in redox signaling*
- 1515 **Pérez-Pérez ME, Florencio FJ, Lindahl M** (2006) Selecting thioredoxins for disulphide
1516 proteomics: target proteomes of three thioredoxins from the cyanobacterium
1517 *Synechocystis* sp. PCC 6803. *Proteomics* **6 Suppl 1**: 186–195
- 1518 **Pérez-Pérez ME, Mauriès A, Maes A, Tourasse NJ, Hamon M, Lemaire SD, Marchand**
1519 **CH** (2017) The Deep Thioredoxome in *Chlamydomonas reinhardtii*: New Insights
1520 into Redox Regulation. *Mol Plant* **10**: 1107–1125
- 1521 **Pérez-Ruiz JM, Guinea M, Puerto-Galán L, Cejudo FJ** (2014) NADPH Thioredoxin
1522 Reductase C Is Involved in Redox Regulation of the Mg-Chelatase I Subunit in
1523 *Arabidopsis thaliana* Chloroplasts. *Mol Plant* **7**: 1252–1255
- 1524 **Pérez-Ruiz JM, Naranjo B, Ojeda V, Guinea M, Cejudo FJ** (2017) NTRC-dependent
1525 redox balance of 2-Cys peroxiredoxins is needed for optimal function of the

- 1526 photosynthetic apparatus. *Proceedings of the National Academy of Sciences* **114**:
1527 12069–12074
- 1528 **Reichheld J-P, Khafif M, Riondet C, Droux M, Bonnard G, Meyer Y** (2007)
1529 Inactivation of thioredoxin reductases reveals a complex interplay between
1530 thioredoxin and glutathione pathways in Arabidopsis development. *Plant Cell* **19**:
1531 1851–1865
- 1532 **Richter AS, Peter E, Rothbart M, Schlicke H, Toivola J, Rintamäki E, Grimm B** (2013)
1533 Posttranslational Influence of NADPH-Dependent Thioredoxin Reductase C on
1534 Enzymes in Tetrapyrrole Synthesis. *Plant Physiol* **162**: 63–73
- 1535 **Scheibe R** (1991) Redox-modulation of chloroplast enzymes: A common principle for
1536 individual control. *Plant Physiol* **96**: 1–3
- 1537 **Schjoerring JK, Mäck G, Nielsen KH, Husted S, Suzuki A, Driscoll S, Boldt R, Bauwe**
1538 **H** (2006) Antisense reduction of serine hydroxymethyltransferase results in
1539 diurnal displacement of NH₄⁺ assimilation in leaves of *Solanum tuberosum*. *Plant*
1540 *Journal* **45**: 71–82
- 1541 **Schürmann P, Buchanan BB** (2008) The ferredoxin/thioredoxin system of oxygenic
1542 photosynthesis. *Antioxid Redox Signal* **10**: 1235–74
- 1543 **Selinski J, Scheibe R** (2019) Malate valves: old shuttles with new perspectives. *Plant*
1544 *Biol* **21**: 21–30
- 1545 **Serrato AJ, Pérez-Ruiz JM, Spínola MC, Cejudo FJ** (2004) A novel NADPH thioredoxin
1546 reductase, localized in the chloroplast, which deficiency causes hypersensitivity to
1547 abiotic stress in *Arabidopsis thaliana*. *J Biol Chem* **279**: 43821–43827
- 1548 **Shin JS, Kim SY, So WM, Noh M, Yoo KS, Shin JS** (2020) Lon domain-containing
1549 protein 1 represses thioredoxin y2 and regulates ROS levels in Arabidopsis
1550 chloroplasts. *FEBS Lett* **594**: 986–994
- 1551 **Simionato D, Basso S, Zaffagnini M, Lana T, Marzotto F, Trost P, Morosinotto T**
1552 (2015) Protein redox regulation in the thylakoid lumen: The importance of
1553 disulfide bonds for violaxanthin de-epoxidase. *FEBS Lett* **589**: 919–923
- 1554 **Somerville CR, Ogren WL** (1980) Inhibition of photosynthesis in. *Nature* **286**: 257–
1555 259
- 1556 **Stöcker S, Maurer M, Ruppert T, Dick TP** (2018) A role for 2-Cys peroxiredoxins in
1557 facilitating cytosolic protein thiol oxidation. *Nat Chem Biol* **14**: 148–155
- 1558 **Suzuki A, Knaff DB** (2005) Glutamate synthase: Structural, mechanistic and regulatory
1559 properties, and role in the amino acid metabolism. *Photosynth Res* **83**: 191–217
- 1560 **Teh JT, Leitz V, Holzer VJC, Neusius D, Marino G, Meitzel T, García-Cerdán JG, Dent**
1561 **RM, Niyogi KK, Geigenberger P, et al** (2023) NTRC regulates CP12 to activate
1562 Calvin–Benson cycle during cold acclimation. *Proceedings of the National Academy*
1563 *of Sciences*. doi: 10.1073/pnas.2306338120
- 1564 **Thormählen I, Meitzel T, Groysman J, Öchsner AB, von Roepenack-Lahaye E,**
1565 **Naranjo B, Cejudo FJ, Geigenberger P** (2015) Thioredoxin f1 and NADPH-
1566 dependent thioredoxin reductase C have overlapping functions in regulating
1567 photosynthetic metabolism and plant growth in response to varying light
1568 conditions. *Plant Physiol* **169**: pp.01122.2015
- 1569 **Thormählen I, Ruber J, Von Roepenack-Lahaye E, Ehrlich SM, Massot V, Hümmer C,**
1570 **Tezycka J, Issakidis-Bourguet E, Geigenberger P** (2013) Inactivation of
1571 thioredoxin f1 leads to decreased light activation of ADP-glucose
1572 pyrophosphorylase and altered diurnal starch turnover in leaves of Arabidopsis
1573 plants. *Plant Cell Environ* **36**: 16–29
- 1574 **Thormählen I, Zupok A, Rescher J, Leger J, Weissenberger S, Groysman J, Orwat A,**
1575 **Chatel-Innocenti G, Issakidis-Bourguet E, Armbruster U, et al** (2017)

- 1576 Thioredoxins Play a Crucial Role in Dynamic Acclimation of Photosynthesis in
1577 Fluctuating Light. *Mol Plant* **10**: 168–182
- 1578 **Topf U, Suppanz I, Samluk L, Wrobel L, Böser A, Sakowska P, Knapp B, Pietrzyk MK,**
1579 **Chacinska A, Warscheid B** (2018) Quantitative proteomics identifies redox
1580 switches for global translation modulation by mitochondrially produced reactive
1581 oxygen species. *Nat Commun.* doi: 10.1038/s41467-017-02694-8
- 1582 **Uhrig RG, Echevarría-Zomeño S, Schlapfer P, Grossmann J, Roschitzki B, Koerber N,**
1583 **Fiorani F, Gruissem W** (2021) Diurnal dynamics of the Arabidopsis rosette
1584 proteome and phosphoproteome. *Plant Cell Environ* **44**: 821–841
- 1585 **Vaseghi M-J, Chibani K, Telman W, Liebthal MF, Gerken M, Schnitzer H, Mueller SM,**
1586 **Dietz K-J** (2018) The chloroplast 2-cysteine peroxiredoxin functions as thioredoxin
1587 oxidase in redox regulation of chloroplast metabolism. *Elife.* doi:
1588 10.7554/eLife.38194
- 1589 **Wang P, Liu J, Liu B, Da Q, Feng D, Su J, Zhang Y, Wang J, Wang H bin** (2014)
1590 Ferredoxin:Thioredoxin reductase is required for proper chloroplast development
1591 and is involved in the regulation of plastid gene expression in Arabidopsis thaliana.
1592 *Mol Plant* **7**: 1586–1590
- 1593 **Wang P, Liu J, Liu B, Feng D, Da Q, Wang P, Shu S, Su J, Zhang Y, Wang J, et al** (2013)
1594 Evidence for a role of chloroplastic m-type thioredoxins in the biogenesis of
1595 photosystem II in arabidopsis. *Plant Physiol* **163**: 1710–1728
- 1596 **Wittmann D, Geigenberger P, Grimm B** (2023) NTRC and TRX-f Coordinately Affect
1597 the Levels of Enzymes of Chlorophyll Biosynthesis in a Light-Dependent Manner.
1598 *Cells* **12**: 1670
- 1599 **Wong JH, Cai N, Balmer Y, Tanaka CK, Vensel WH, Hurkman WJ, Buchanan BB**
1600 (2004) Thioredoxin targets of developing wheat seeds identified by
1601 complementary proteomic approaches. *Phytochemistry* **65**: 1629–1640
- 1602 **Yamamoto HY, Kamite L** (1972) The effects of dithiothreitol on violaxanthin de-
1603 epoxidation and absorbance changes in the 500-nm region. *Biochimica et*
1604 *Biophysica Acta (BBA) - Bioenergetics* **267**: 538–543
- 1605 **Yamazaki D, Motohashi K, Kasama T, Hara Y, Hisabori T** (2004) Target Proteins of
1606 the Cytosolic Thioredoxins in Arabidopsis thaliana. *Plant Cell Physiol* **45**: 18–27
- 1607 **Yano H, Wong JH, Lee YM, Cho MJ, Buchanan BB** (2001) A strategy for the
1608 identification of proteins targeted by thioredoxin. *Proc Natl Acad Sci U S A* **98**:
1609 4794–4799
- 1610 **Yoshida K, Hara S, Hisabori T** (2015) Thioredoxin selectivity for thiol-based redox
1611 regulation of target Proteins in Chloroplasts. *Journal of Biological Chemistry* **290**:
1612 14278–14288
- 1613 **Yoshida K, Hisabori T** (2016) Two distinct redox cascades cooperatively regulate
1614 chloroplast functions and sustain plant viability. *Proceedings of the National*
1615 *Academy of Sciences* **113**: E3967–E3976
- 1616 **Yoshida K, Noguchi K, Motohashi K, Hisabori T** (2013) Systematic exploration of
1617 thioredoxin target proteins in plant mitochondria. *Plant Cell Physiol* **54**: 875–892
- 1618 **Yoshida K, Yokochi Y, Tanaka K, Hisabori T** (2022) The ferredoxin/thioredoxin
1619 pathway constitutes an indispensable redox-signaling cascade for light-dependent
1620 reduction of chloroplast stromal proteins. *Journal of Biological Chemistry* **298**:
1621 102650
- 1622 **Yu A, Xie Y, Pan X, Zhang H, Cao P, Su X, Chang W, Li M** (2020) Photosynthetic
1623 Phosphoribulokinase Structures: Enzymatic Mechanisms and the Redox Regulation
1624 of the Calvin-Benson-Bassham Cycle. *Plant Cell* **32**: 1556–1573
- 1625 **Zaffagnini M, Fermani S, Marchand CH, Costa A, Sparla F, Rouhier N, Geigenberger**
1626 **P, Lemaire SD, Trost P** (2019) Redox Homeostasis in Photosynthetic Organisms:

1627 Novel and Established Thiol-Based Molecular Mechanisms. Antioxid Redox Signal
1628 **31**: 155–210
1629 **Zimmer D, Swart C, Graf A, Arrivault S, Tillich M, Proost S, Nikoloski Z, Stitt M,**
1630 **Bock R, Mühlhaus T, et al** (2021) Topology of the redox network during induction
1631 of photosynthesis as revealed by time-resolved proteomics in tobacco. Sci Adv. doi:
1632 10.1126/sciadv.abi8307
1633

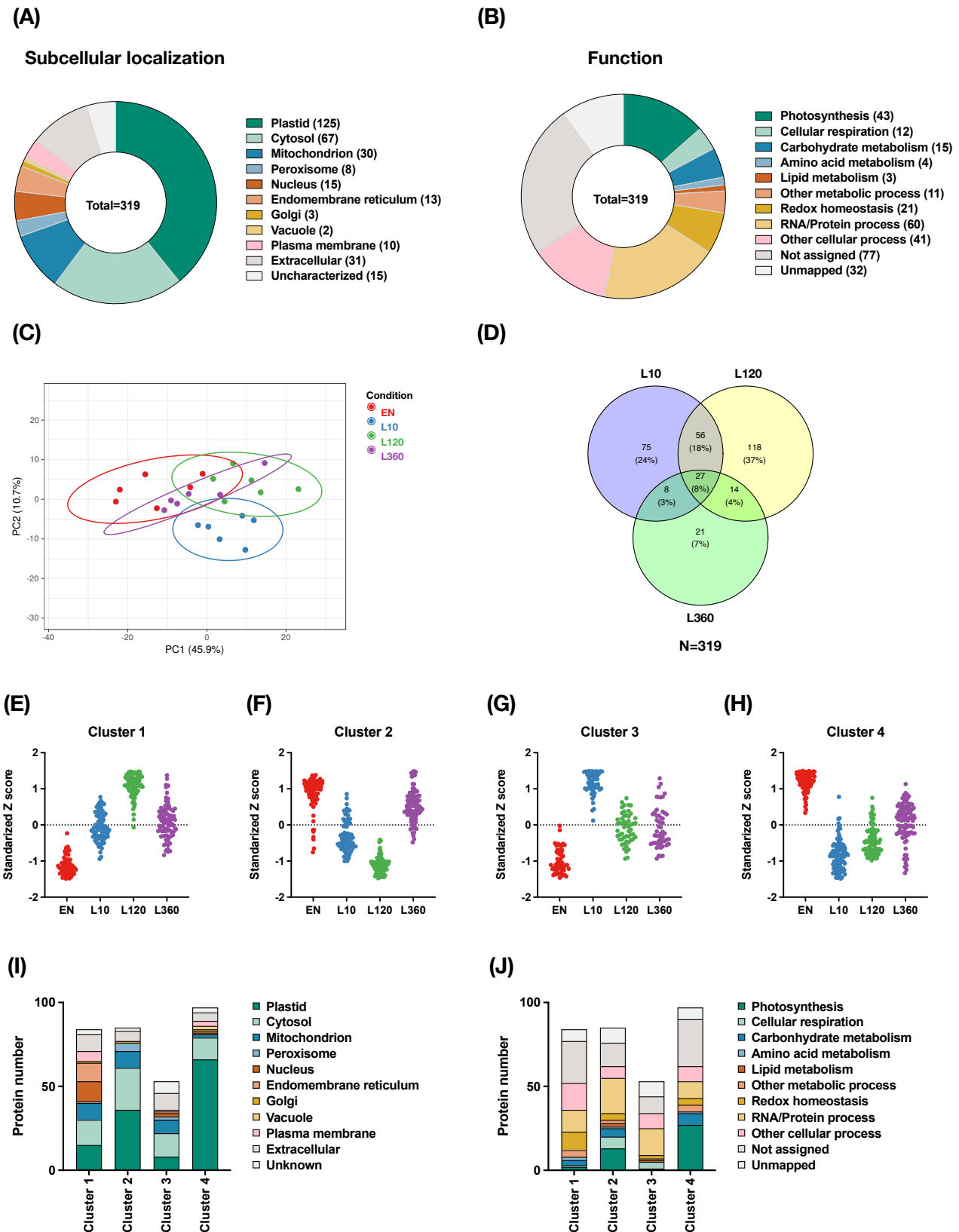


Figure 1. Light-dependent dynamics in the landscape of protein-oxidation changes at different time points into the photoperiod. Redox proteomics analyses of Arabidopsis plants sampled 10 (L10), 120 (L120) and 360 min (L360) into the photoperiod, compared to end of the night (EN, dark conditions). (A) Subcellular localization of proteins showing significant changes in their oxidation levels in the light, compared to the dark. (B) Functional categories of proteins showing significant changes in their oxidation levels in the light, compared to the dark. (C) Principal component analysis displaying the distinctions of protein oxidation states between EN, and L10, L120 and L360. (D) Venn diagram highlighting the distribution of proteins subject to significant changes in oxidation states at different time points into the photoperiod, compared to EN. (E) - (H) Unsupervised cluster analysis showing the grouping of proteins that display different redox changes in response to a time course in the light. (I) The subcellular localization of proteins from the different clusters. (J) The biological function categories of proteins from the different clusters. Data are based on three to six biological replicates.

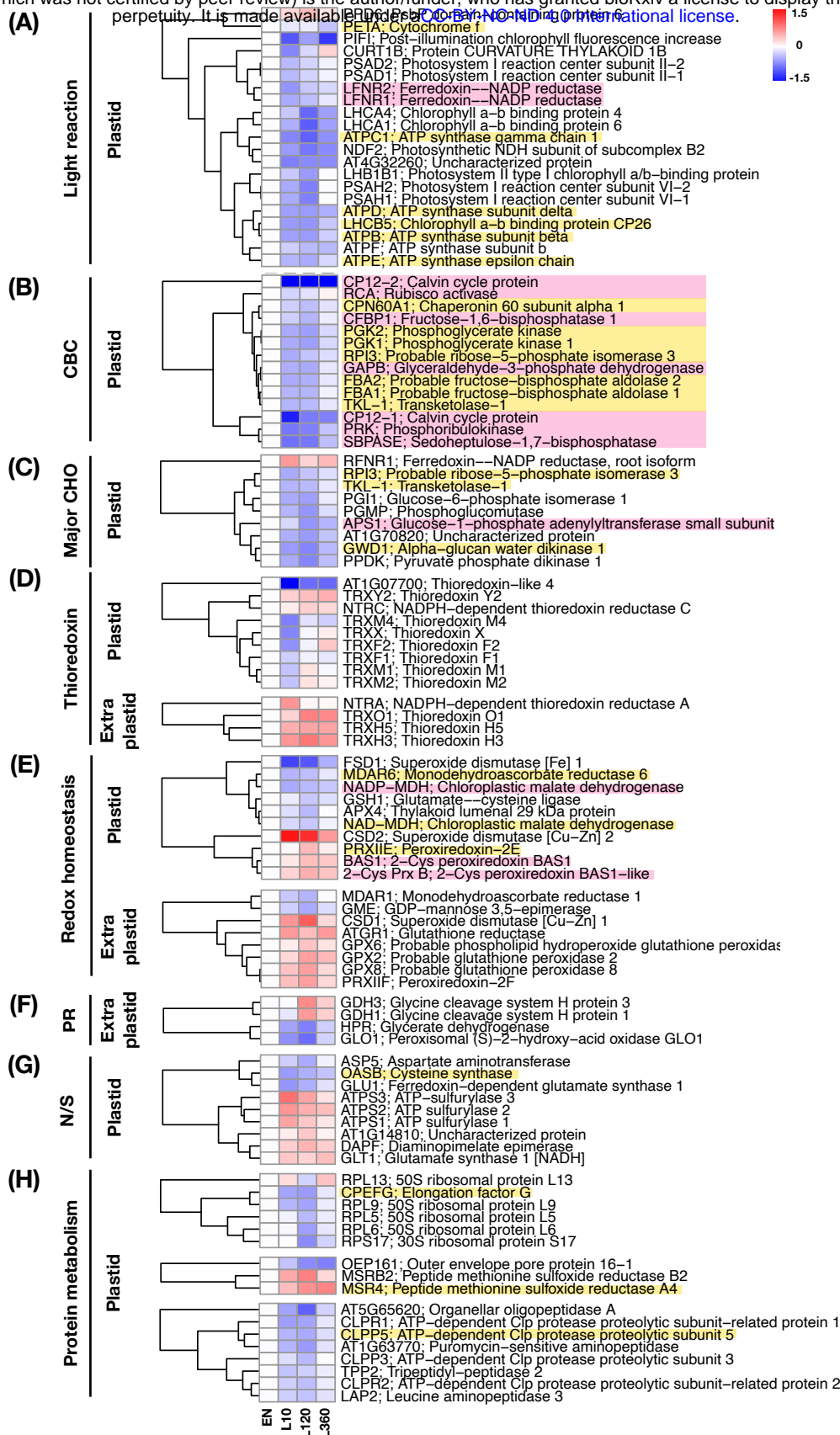


Figure 2. Protein-oxidation changes in photosynthetic processes, redox balance, metabolic pathways and protein metabolism in response to light. The heatmaps summarize the log₂ fold changes of protein oxidation levels at 10 (L10), 120 (L120) and 360 min (L360) into the photoperiod, relative to the end of the night (EN, dark conditions). Proteins were allocated to different groups of biological functions including (A) light reaction, (B) Calvin Benson Cycle (CBC), (C) major carbohydrate (CHO) metabolism, (D) thioredoxin, (E) redox homeostasis, (F) photorespiration (PR), (G) nitrogen and sulfur metabolism (N/S) and (H) protein metabolism. The protein metabolism group is further divided in to three subgroups including synthesis, modification and degradation (from up to down). Data are the means of three to six biological replicates. The proteins high-lighted with pink background are validated Trx targets, while those with yellow background have been proposed to be redox-regulated proteins according to previous studies (Lindahl and Kieselbach, 2009). red = increased oxidation, blue = decreased oxidation. Raw data and statistics, see Supplemental Table S1.

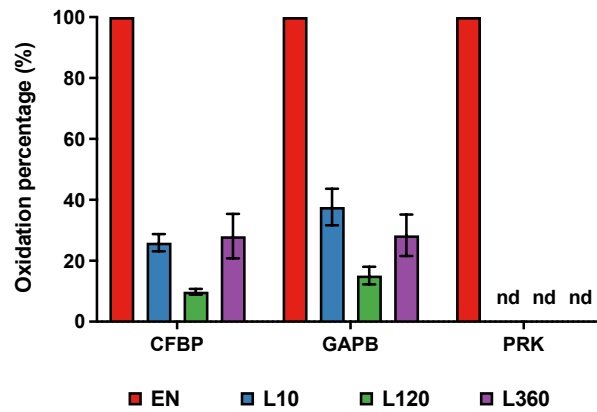


Figure 3. Validation of the redox proteomics results by analyzing oxidation percentages of CBC enzymes using protein electrophoretic mobility shift assays as an independent method. The protein oxidation percentages of chloroplastic fructose 1,6-bisphosphatase (CFBP), glyceraldehyde-3-phosphate dehydrogenase B (GAPB) and phosphoribulokinase (PRK) were analyzed via protein electrophoretic mobility shift assay as an independent method. For three independent biological replicates, the reduced thiols of proteins were alkylated using NEM, and the oxidized thiols of proteins were released by treating with DTT. The released thiols were further labeled with methoxypolyethylene glycol maleimide, which resulted in an increase of protein mass of the oxidized form that became distinguishable from the reduced form during gel electrophoresis. The oxidation percentages of CFBP, GAPB and PRK were calculated from the scanned blots shown in Supplemental Figure S2 by dividing the intensities of the bands reflecting the oxidized form by the sum of the intensities of the bands reflecting oxidized plus reduced forms of the respective protein. Results are means \pm SE (n=3). The symbol “nd” indicates “not detectable”.

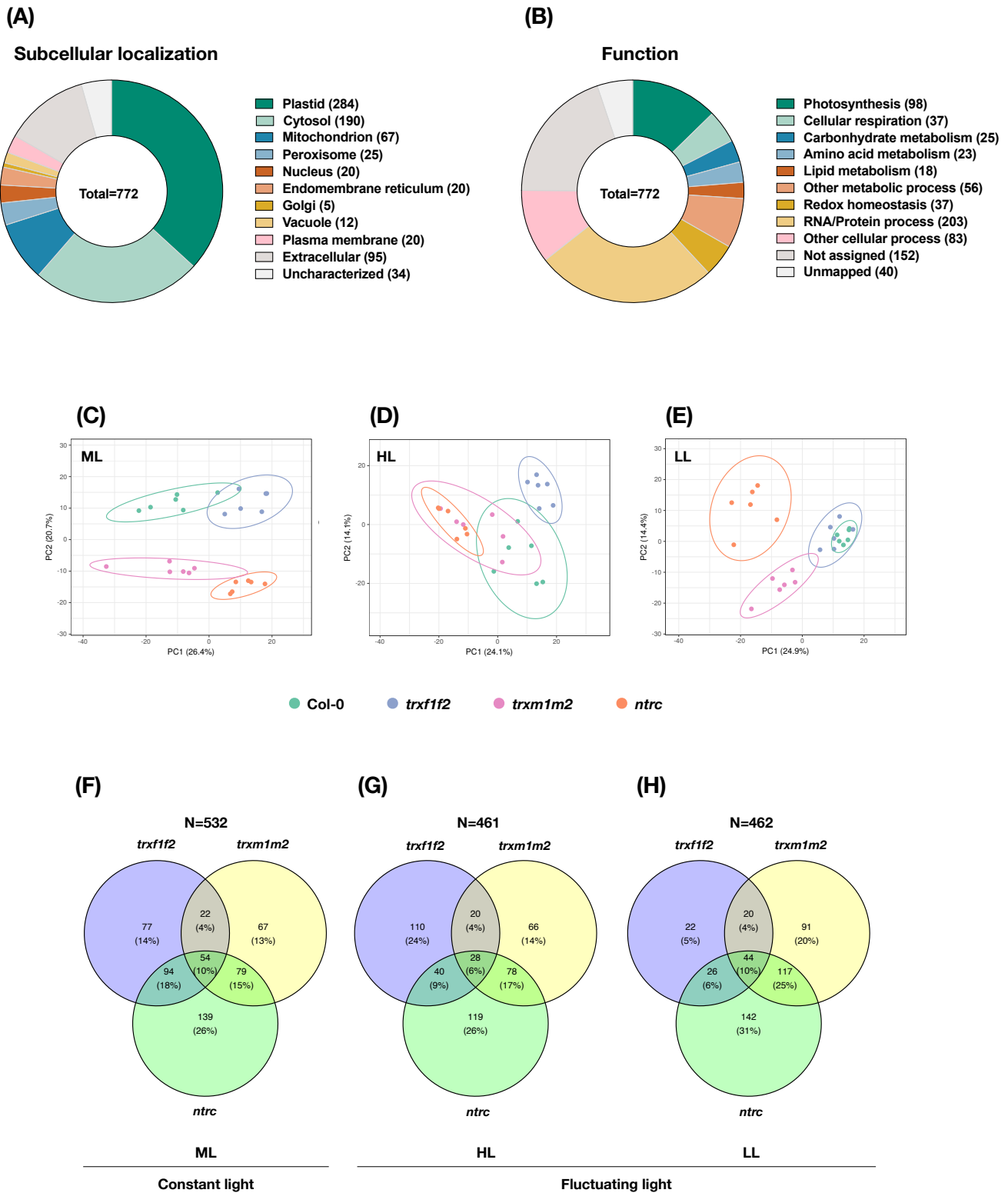


Figure 4. Dynamics in the landscape of protein oxidation changes across mutants lacking different parts of NTRC/Trx systems in constant and fluctuating light. Redox proteomics analyses of *Arabidopsis* *trx1f2*, *trx1m2* or *ntrc* mutants relative to the wild type (Col-0). Plants were grown in the same conditions as in Figures 1-3 (ML = medium light) or in fluctuating light (FL) with rapidly alternating high light (HL, 1 min) and low light (LL, 5 min) phases. Samples were taken 360 min into the photoperiod. (A) The subcellular localization of proteins showing significantly different oxidation states in the mutants relative to the wild type. (B) The functional categories of proteins showing significantly different oxidation states in the mutants relative to the wild type. (C) - (E) The principal component analysis displaying the distinctions of protein oxidation states between wild type (Col-0), *trx1f2*, *trx1m2* and *ntrc* mutants in ML or in HL or LL phases of FL. (F) - (H) Venn diagram highlighting the distribution of proteins subject to marked changes in their oxidation states in the respective mutants, compared to the wild type, during constant ML, as well as during HL or LL phases of FL. Data are based on three to six biological replicates.

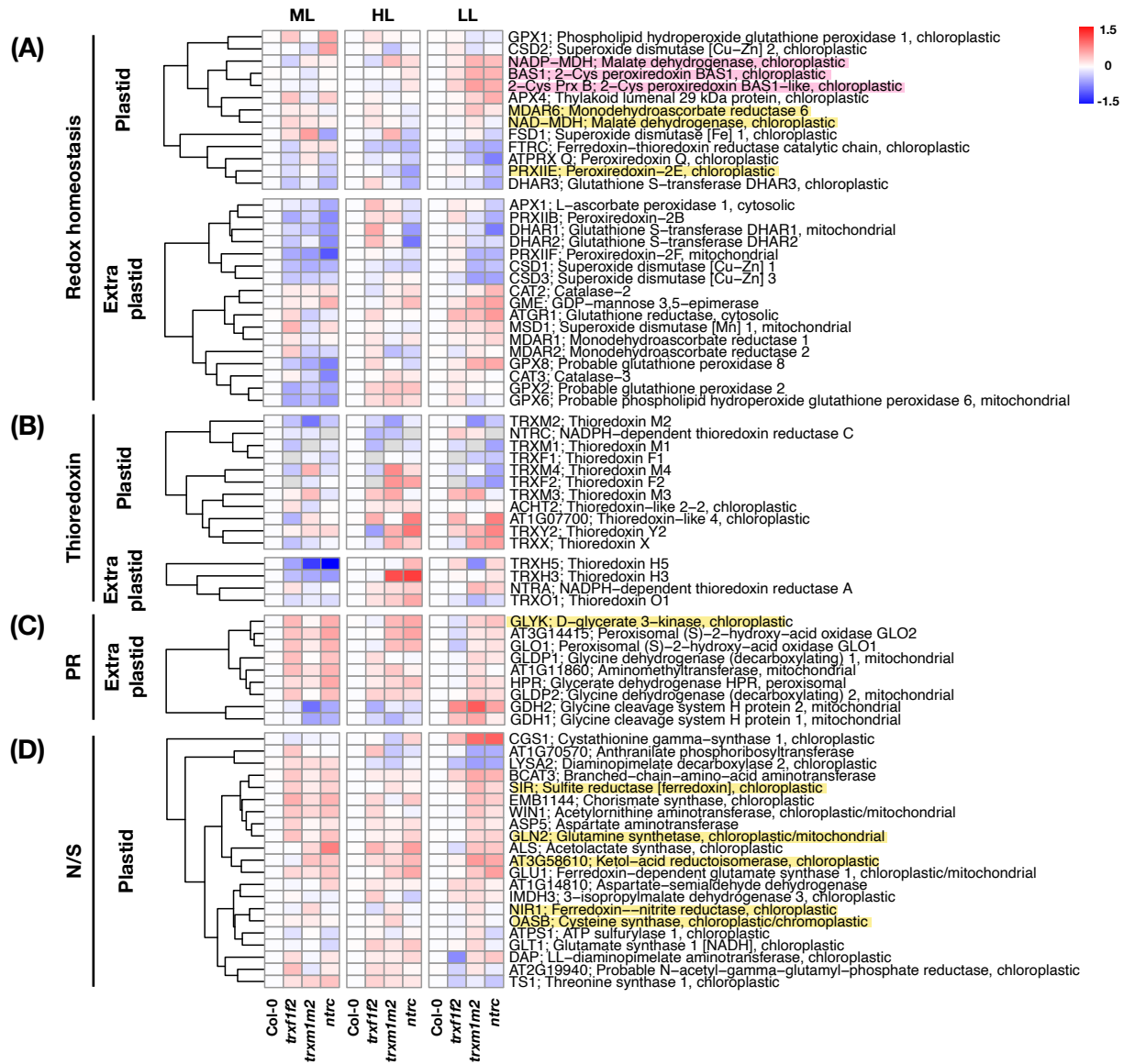


Figure 6. Protein oxidation changes in redox homeostasis, photorespiration and amino acid metabolism across *trxf1f2*, *trxm1m2* and *ntrc* mutants in constant and fluctuating light. Heatmaps summarize the \log_2 fold changes of protein oxidation levels in Arabidopsis *trxf1f2*, *trxm1m2* or *ntrc* mutants relative to the wild type (Col-0). The proteins highlighted with pink background are validated Trx targets, while those with yellow background have been proposed to be redox-regulated proteins according to previous studies (Lindahl and Kieselbach, 2009). Proteins were allocated to different groups of biological functions including (A) redox homeostasis, (B) thioredoxin (C) photorespiration (PR) and (D) nitrogen and sulfur metabolism (N/S). Plants were grown in the same conditions as indicated in the legend to Figure 4. Data are the means of three to six biological replicates. ML, medium light; FL, fluctuating light; HL, high-light phase of FL; LL, low-light phase of FL; red = increased oxidation, blue = decreased oxidation. Raw data and statistics, see Supplemental Table S4.

Parsed Citations

Albrecht V, Ingenfeld A, Apel K (2006) Characterization of the snowy cotyledon 1 mutant of *Arabidopsis thaliana*: The impact of chloroplast elongation factor G on chloroplast development and plant vitality. *Plant Mol Biol* 60: 507–518

Google Scholar: [Author Only](#) [Title Only](#) [Author and Title](#)

Alkhalfioui F, Renard M, Montrichard F (2007) Unique properties of NADP-thioredoxin reductase C in legumes. *J Exp Bot*. doi: 10.1093/jxb/erl248

Google Scholar: [Author Only](#) [Title Only](#) [Author and Title](#)

Arsova B, Hoja U, Wimmelbacher M, Greiner E, Üstün Ş, Melzer M, Petersen K, Lein W, Börnke F (2010) Plastidial thioredoxin z interacts with two fructokinase-like proteins in a thiol-dependent manner: Evidence for an essential role in chloroplast development in *Arabidopsis* and *Nicotiana benthamiana*. *Plant Cell* 22: 1498–1515

Google Scholar: [Author Only](#) [Title Only](#) [Author and Title](#)

Balmer Y, Koller A, Del Val G, Manieri W, Schürmann P, Buchanan BB (2003) Proteomics gives insight into the regulatory function of chloroplast thioredoxins. *Proc Natl Acad Sci U S A* 100: 370–375

Google Scholar: [Author Only](#) [Title Only](#) [Author and Title](#)

Balmer Y, Vensel WH, Hurkman WJ, Buchanan BB (2006) Thioredoxin Target Proteins in Chloroplast Thylakoid Membranes. *Antioxid Redox Signal* 8: 1829–1834

Google Scholar: [Author Only](#) [Title Only](#) [Author and Title](#)

Balmer Y, Vensel WH, Tanaka CK, Hurkman WJ, Gelhaye E, Rouhier N, Jacquot JP, Manieri W, Schürmann P, Droux M, et al (2004a) Thioredoxin links redox to the regulation of fundamental processes of plant mitochondria. *Proc Natl Acad Sci U S A* 101: 2642–2647

Google Scholar: [Author Only](#) [Title Only](#) [Author and Title](#)

Balmer Y, Vensel WH, Tanaka CK, Hurkman WJ, Gelhaye E, Rouhier N, Jacquot J-P, Manieri W, Schürmann P, Droux M, et al (2004b) Thioredoxin links redox to the regulation of fundamental processes of plant mitochondria. *Proceedings of the National Academy of Sciences* 101: 2642–2647

Google Scholar: [Author Only](#) [Title Only](#) [Author and Title](#)

Bartsch S, Monnet J, Selbach K, Quigley F, Gray J, Von Wettstein D, Reinbothe S, Reinbothe C (2008) Three thioredoxin targets in the inner envelope membrane of chloroplasts function in protein import and chlorophyll metabolism. *Proc Natl Acad Sci U S A* 105: 4933–4938

Google Scholar: [Author Only](#) [Title Only](#) [Author and Title](#)

Bashandy T, Taconnat L, Renou JP, Meyer Y, Reichheld JP (2009) Accumulation of flavonoids in an ntra ntrb mutant leads to tolerance to UV-C. *Mol Plant* 2: 249–258

Google Scholar: [Author Only](#) [Title Only](#) [Author and Title](#)

Bohrer AS, Massot V, Innocenti G, Reichheld JP, Issakidis-Bourguet E, Vanacker H (2012) New insights into the reduction systems of plastidial thioredoxins point out the unique properties of thioredoxin z from *Arabidopsis*. *J Exp Bot* 63: 6315–6323

Google Scholar: [Author Only](#) [Title Only](#) [Author and Title](#)

Brandes HK, Larimer FW, Geck MK, Stringer CD, Schürmann P, Hartman FC (1993) Direct identification of the primary nucleophile of thioredoxin f. *Journal of Biological Chemistry* 268: 18411–18414

Google Scholar: [Author Only](#) [Title Only](#) [Author and Title](#)

Carrillo LR, Froehlich JE, Cruz JA, Savage LJ, Kramer DM (2016) Multi-level regulation of the chloroplast ATP synthase: The chloroplast NADPH thioredoxin reductase C (NTRC) is required for redox modulation specifically under low irradiance. *The Plant Journal* 87: 654–663

Google Scholar: [Author Only](#) [Title Only](#) [Author and Title](#)

Cejudo FJ, Ferrández J, Cano B, Puerto-Galán L, Guinea M (2012) The function of the NADPH thioredoxin reductase C-2-Cys peroxiredoxin system in plastid redox regulation and signalling. *FEBS Lett* 586: 2974–2980

Google Scholar: [Author Only](#) [Title Only](#) [Author and Title](#)

Cejudo FJ, González MC, Pérez-Ruiz JM (2021) Redox regulation of chloroplast metabolism. *Plant Physiol* 186: 9–21

Google Scholar: [Author Only](#) [Title Only](#) [Author and Title](#)

Cejudo FJ, Ojeda V, Delgado-Requerey V, González M, Pérez-Ruiz JM (2019) Chloroplast redox regulatory mechanisms in plant adaptation to light and darkness. *Front Plant Sci* 10: 1–11

Google Scholar: [Author Only](#) [Title Only](#) [Author and Title](#)

Cha JY, Kim JY, Jung IJ, Kim MR, Melencion A, Alam SS, Yun DJ, Lee SY, Kim MG, Kim WY (2014) NADPH-dependent thioredoxin reductase A (NTRA) confers elevated tolerance to oxidative stress and drought. *Plant Physiology and Biochemistry* 80: 184–191

Google Scholar: [Author Only](#) [Title Only](#) [Author and Title](#)

Chen Q, Xiao Y, Ming Y, Peng R, Hu J, Wang H, Jin H (2022) Quantitative proteomics reveals redox-based functional regulation of photosynthesis under fluctuating light in plants. *J Integr Plant Biol* 64: 2168–2186

Google Scholar: [Author Only](#) [Title Only](#) [Author and Title](#)

Collin V, Issakidis-Bourguet E, Marchand C, Hirasawa M, Lancelin JM, Knaff DB, Miginiac-Maslow M (2003) The Arabidopsis plastidial thioredoxins. New functions and new insights into specificity. *Journal of Biological Chemistry* 278: 23747–23752

Google Scholar: [Author Only](#) [Title Only](#) [Author and Title](#)

Collin V, Lamkemeyer P, Miginiac-Maslow M, Hirasawa M, Knaff DB, Dietz KJ, Issakidis-Bourguet E (2004) Characterization of plastidial thioredoxins from Arabidopsis belonging to the new γ -type. *Plant Physiol* 136: 4088–4095

Google Scholar: [Author Only](#) [Title Only](#) [Author and Title](#)

Coruzzi GM (2003) Primary N-assimilation into Amino Acids in Arabidopsis. *Arabidopsis Book* 2: e0010

Google Scholar: [Author Only](#) [Title Only](#) [Author and Title](#)

Coschigano KT, Melo-Oliveira R, Lim J, Coruzzi GM (1998) Arabidopsis gls mutants and distinct Fd-GOGAT genes: Implications for photorespiration and primary nitrogen assimilation. *Plant Cell* 10: 741–752

Google Scholar: [Author Only](#) [Title Only](#) [Author and Title](#)

Cox J, Mann M (2008) MaxQuant enables high peptide identification rates, individualized p.p.b.-range mass accuracies and proteome-wide protein quantification. *Nat Biotechnol* 26: 1367–1372

Google Scholar: [Author Only](#) [Title Only](#) [Author and Title](#)

Cremers CM, Jakob U (2013) Oxidant sensing by reversible disulfide bond formation. *Journal of Biological Chemistry* 288: 26489–26496

Google Scholar: [Author Only](#) [Title Only](#) [Author and Title](#)

Da Q, Sun T, Wang M, Jin H, Li M, Feng D, Wang J, Wang H Bin, Liu B (2018) M-type thioredoxins are involved in the xanthophyll cycle and proton motive force to alter NPQ under low-light conditions in Arabidopsis. *Plant Cell Rep* 37: 279–291

Google Scholar: [Author Only](#) [Title Only](#) [Author and Title](#)

Da Q, Wang P, Wang M, Sun T, Jin H, Liu B, Wang J, Grimm B, Wang H-B (2017) Thioredoxin and NADPH-dependent thioredoxin reductase C regulation of Tetrapyrrole Biosynthesis. *Plant Physiol* 175: 652–666

Google Scholar: [Author Only](#) [Title Only](#) [Author and Title](#)

Delgado-Requerey V, Cejudo FJ, González M-C (2023) The Functional Relationship between NADPH Thioredoxin Reductase C, 2-Cys Peroxiredoxins, and m-Type Thioredoxins in the Regulation of Calvin–Benson Cycle and Malate-Valve Enzymes in Arabidopsis. *Antioxidants* 12: 1041

Google Scholar: [Author Only](#) [Title Only](#) [Author and Title](#)

Dietz KJ, Hell R (2015) Thiol switches in redox regulation of chloroplasts: Balancing redox state, metabolism and oxidative stress. *Biol Chem* 396: 483–494

Google Scholar: [Author Only](#) [Title Only](#) [Author and Title](#)

Dziubek D, Poeker L, Siemiątkowska B, Graf A, Marino G, Alseekh S, Arrivault S, Fernie AR, Armbruster U, Geigenberger P (2023) NTRC and thioredoxins m1/ m2 underpin the light acclimation of plants on proteome and metabolome levels. *Plant Physiol*. doi: 10.1093/plphys/kiad535

Google Scholar: [Author Only](#) [Title Only](#) [Author and Title](#)

Fernández-Marín B, Roach T, Verhoeven A, García-Plazaola JI (2021) Shedding light on the dark side of xanthophyll cycles. *New Phytologist* 230: 1336–1344

Google Scholar: [Author Only](#) [Title Only](#) [Author and Title](#)

Geigenberger P, Thormählen I, Daloso DM, Fernie AR (2017) The Unprecedented Versatility of the Plant Thioredoxin System. *Trends Plant Sci* 22: 249–262

Google Scholar: [Author Only](#) [Title Only](#) [Author and Title](#)

Goyer A, Haslekås C, Miginiac-Maslow M, Klein U, Le Marechal P, Jacquot JP, Decottignies P (2002) Isolation and characterization of a thioredoxin-dependent peroxidase from *Chlamydomonas reinhardtii*. *Eur J Biochem* 269: 272–282

Google Scholar: [Author Only](#) [Title Only](#) [Author and Title](#)

Guinea Diaz M, Nikkanen L, Himanen K, Toivola J, Rintamäki E (2020) Two chloroplast thioredoxin systems differentially modulate photosynthesis in Arabidopsis depending on light intensity and leaf age. *Plant Journal* 104: 718–734

Google Scholar: [Author Only](#) [Title Only](#) [Author and Title](#)

Hall M, Mata-Cabana A, Åkerlund HE, Florencio FJ, Schröder WP, Lindahl M, Kieselbach T (2010) Thioredoxin targets of the plant chloroplast lumen and their implications for plastid function. *Proteomics* 10: 987–1001

Google Scholar: [Author Only](#) [Title Only](#) [Author and Title](#)

Hammel A, Zimmer D, Sommer F, Mühlhaus T, Schroda M (2018) Absolute Quantification of Major Photosynthetic Protein

Complexes in *Chlamydomonas reinhardtii* Using Quantification Concatamers (QconCATs). *Front Plant Sci.* doi: 10.3389/fpls.2018.01265

Google Scholar: [Author Only](#) [Title Only](#) [Author and Title](#)

Hanke GT, Okutani S, Satomi Y, Takao T, Suzuki A, Hase T (2005) Multiple iso-proteins of FNR in Arabidopsis: Evidence for different contributions to chloroplast function and nitrogen assimilation. *Plant Cell Environ* 28: 1146–1157

Google Scholar: [Author Only](#) [Title Only](#) [Author and Title](#)

Havaux M, Dall'Osto L, Bassi R (2007) Zeaxanthin Has Enhanced Antioxidant Capacity with Respect to All Other Xanthophylls in Arabidopsis Leaves and Functions Independent of Binding to PSII Antennae. *Plant Physiol* 145: 1506–1520

Google Scholar: [Author Only](#) [Title Only](#) [Author and Title](#)

Heber UW, Santarius KA (1965) Compartmentation and reduction of pyridine nucleotides in relation to photosynthesis. *Biochim Biophys Acta* 109: 390–408

Google Scholar: [Author Only](#) [Title Only](#) [Author and Title](#)

Hieber AD, Bugos RC, Yamamoto HY (2000) Plant lipocalins: violaxanthin de-epoxidase and zeaxanthin epoxidase. *Biochimica et Biophysica Acta (BBA) - Protein Structure and Molecular Enzymology* 1482: 84–91

Google Scholar: [Author Only](#) [Title Only](#) [Author and Title](#)

Holmgren A (1995) Thioredoxin structure and mechanism: conformational changes on oxidation of the active-site sulfhydryls to a disulfide. *Structure* 3: 239–243

Google Scholar: [Author Only](#) [Title Only](#) [Author and Title](#)

Hooper CM, Castleden IR, Tanz SK, Aryamanesh N, Millar AH (2017) SUBA4: the interactive data analysis centre for Arabidopsis subcellular protein locations. *Nucleic Acids Res* 45: D1064–D1074

Google Scholar: [Author Only](#) [Title Only](#) [Author and Title](#)

Hou LY, Lehmann M, Geigenberger P (2021) Thioredoxin h2 and o1 show different subcellular localizations and redox-active functions, and are extrachloroplastic factors influencing photosynthetic performance in fluctuating light. *Antioxidants.* doi: 10.3390/antiox10050705

Google Scholar: [Author Only](#) [Title Only](#) [Author and Title](#)

Jacquot JP, Eklund H, Rouhier N, Schürmann P (2009) Structural and evolutionary aspects of thioredoxin reductases in photosynthetic organisms. *Trends Plant Sci* 14: 336–343

Google Scholar: [Author Only](#) [Title Only](#) [Author and Title](#)

Jaffrey SR, Snyder SH (2001) The Biotin Switch Method for the Detection of S -Nitrosylated Proteins. *Science's STKE.* doi: 10.1126/stke.2001.86.pl1

Google Scholar: [Author Only](#) [Title Only](#) [Author and Title](#)

Jurado-Flores A, Delgado-Requerey V, Gálvez-Ramírez A, Puerto-Galán L, Pérez-Ruiz JM, Cejudo FJ (2020) Exploring the functional relationship between ytype thioredoxins and 2-cys peroxiredoxins in arabidopsis chloroplasts. *Antioxidants* 9: 1–18

Google Scholar: [Author Only](#) [Title Only](#) [Author and Title](#)

Kang Z, Qin T, Zhao Z (2019) Thioredoxins and thioredoxin reductase in chloroplasts: A review. *Gene* 706: 32–42

Google Scholar: [Author Only](#) [Title Only](#) [Author and Title](#)

Kirchsteiger K, Pulido P, Gonzálezlez M, Cejudo FJ (2009) NADPH Thioredoxin reductase C controls the redox status of chloroplast 2-Cys peroxiredoxins in arabidopsis thaliana. *Mol Plant* 2: 298–307

Google Scholar: [Author Only](#) [Title Only](#) [Author and Title](#)

Kojima K, Motohashi K, Morota T, Oshita M, Hisabori T, Hayashi H, Nishiyama Y (2009) Regulation of translation by the Redox State of Elongation factor G in the cyanobacterium *Synechocystis* sp. PCC 6803. *Journal of Biological Chemistry* 284: 18685–18691

Google Scholar: [Author Only](#) [Title Only](#) [Author and Title](#)

Laemmli UK (1970) Cleavage of structural proteins during the assembly of the head of bacteriophage T4. *Nature* 227: 680–685

Google Scholar: [Author Only](#) [Title Only](#) [Author and Title](#)

Lamkemeyer P, Laxa M, Collin V, Li W, Finkemeier I, Schöttler MA, Holtkamp V, Tognetti VB, Issakidis-Bourguet E, Kandlbinder A, et al (2006) Peroxiredoxin Q of Arabidopsis thaliana is attached to the thylakoids and functions in context of photosynthesis. *Plant Journal* 45: 968–981

Google Scholar: [Author Only](#) [Title Only](#) [Author and Title](#)

Lamp N, Lev R, Nissan I, Gilad G, Hipsch M, Rosenwasser S (2022) Systematic monitoring of 2-Cys peroxiredoxin-derived redox signals unveiled its role in attenuating carbon assimilation rate. *Proc Natl Acad Sci U S A* 119: 1–10

Google Scholar: [Author Only](#) [Title Only](#) [Author and Title](#)

Lemaire SD, Guillont B, Le Maréchal P, Keryer E, Miginiac-Maslow M, Decottignies P (2004) New thioredoxin targets in the unicellular photosynthetic eukaryote *Chlamydomonas reinhardtii*. *Proc Natl Acad Sci U S A* 101: 7475–7480

Google Scholar: [Author Only](#) [Title Only](#) [Author and Title](#)

Lepistö A, Pakula E, Toivola J, Krieger-Liszak A, Vignols F, Rintamäki E (2013) Deletion of chloroplast NADPH-dependent thioredoxin reductase results in inability to regulate starch synthesis and causes stunted growth under short-day photoperiods. *J Exp Bot* 64: 3843–3854

Google Scholar: [Author Only](#) [Title Only](#) [Author and Title](#)

Lichter A, Haberlein I (1998) A light-dependent redox signal participates in the regulation of ammonia fixation in chloroplasts of higher plants - Ferredoxin: Glutamate synthase is a thioredoxin-dependent enzyme. *J Plant Physiol* 153: 83–90

Google Scholar: [Author Only](#) [Title Only](#) [Author and Title](#)

Lindahl M, Florencio FJ (2003) Thioredoxin-linked processes in cyanobacteria are as numerous as in chloroplasts, but targets are different. *Proc Natl Acad Sci U S A* 100: 16107–16112

Google Scholar: [Author Only](#) [Title Only](#) [Author and Title](#)

Lindahl M, Kieselbach T (2009) Disulphide proteomes and interactions with thioredoxin on the track towards understanding redox regulation in chloroplasts and cyanobacteria. *J Proteomics* 72: 416–438

Google Scholar: [Author Only](#) [Title Only](#) [Author and Title](#)

Liu P, Zhang H, Wang H, Xia Y (2014) Identification of redox-sensitive cysteines in the arabidopsis proteome using OxiTRAQ, a quantitative redox proteomics method. *Proteomics* 14: 750–762

Google Scholar: [Author Only](#) [Title Only](#) [Author and Title](#)

Löwe O, Rezende F, Heidler J, Wittig I, Helfinger V, Brandes RP, Schröder K (2019) BIAM switch assay coupled to mass spectrometry identifies novel redox targets of NADPH oxidase 4. *Redox Biol* 21: 101125

Google Scholar: [Author Only](#) [Title Only](#) [Author and Title](#)

Makmura L, Hamann M, Areopagita A, Furuta S, Muñoz A, Momand J (2001) Development of a Sensitive Assay to Detect Reversibly Oxidized Protein Cysteine Sulfhydryl Groups. *Antioxid Redox Signal* 3: 1105–1118

Google Scholar: [Author Only](#) [Title Only](#) [Author and Title](#)

Marchand C, Le Maréchal P, Meyer Y, Decottignies P (2006) Comparative proteomic approaches for the isolation of proteins interacting with thioredoxin. *Proteomics* 6: 6528–6537

Google Scholar: [Author Only](#) [Title Only](#) [Author and Title](#)

Marchand CH, Vanacker H, Collin V, Issakidis-Bourguet E, Le Maréchal P, Decottignies P (2010) Thioredoxin targets in *Arabidopsis* roots. *Proteomics* 10: 2418–2428

Google Scholar: [Author Only](#) [Title Only](#) [Author and Title](#)

McFarlane CR, Shah NR, Kabasakal B V., Echeverria B, Cotton CAR, Bubeck D, Murray JW (2019) Structural basis of light-induced redox regulation in the Calvin–Benson cycle in cyanobacteria. *Proceedings of the National Academy of Sciences* 116: 20984–20990

Google Scholar: [Author Only](#) [Title Only](#) [Author and Title](#)

Metsalu T, Vilo J (2015) ClustVis: a web tool for visualizing clustering of multivariate data using Principal Component Analysis and heatmap. *Nucleic Acids Res* 43: W566–W570

Google Scholar: [Author Only](#) [Title Only](#) [Author and Title](#)

Meyer Y, Belin C, Delorme-Hinoux V, Reichheld J-P, Riondet C (2012) Thioredoxin and glutaredoxin systems in plants: Molecular mechanisms, crosstalks, and functional significance. *Antioxid Redox Signal* 17: 1124–1160

Google Scholar: [Author Only](#) [Title Only](#) [Author and Title](#)

Michalska J, Zauber H, Buchanan BB, Cejudo FJ, Geigenberger P (2009) NTRC links built-in thioredoxin to light and sucrose in regulating starch synthesis in chloroplasts and amyloplasts. *Proceedings of the National Academy of Sciences* 106: 9908–9913

Google Scholar: [Author Only](#) [Title Only](#) [Author and Title](#)

Michelet L, Lemaire SD, Marchand CH, Fermani S, Sparla F, Morisse S, Pérez-Pérez ME, Trost P, Zaffagnini M, Danon A, et al (2013) Redox regulation of the Calvin–Benson cycle: something old, something new. *Front Plant Sci* 4: 1–21

Google Scholar: [Author Only](#) [Title Only](#) [Author and Title](#)

Miesak BH, Coruzzi GM (2002) Molecular and physiological analysis of *Arabidopsis* mutants defective in cytosolic or chloroplastic aspartate aminotransferase. *Plant Physiol* 129: 650–660

Google Scholar: [Author Only](#) [Title Only](#) [Author and Title](#)

Montrichard F, Alkhalifioui F, Yano H, Vensel WH, Hurkman WJ, Buchanan BB (2009) Thioredoxin targets in plants: The first 30 years. *J Proteomics* 72: 452–474

Google Scholar: [Author Only](#) [Title Only](#) [Author and Title](#)

Moore M, Gossmann N, Dietz KJ (2016) Redox Regulation of Cytosolic Translation in Plants. *Trends Plant Sci* 21: 388–397

Google Scholar: [Author Only](#) [Title Only](#) [Author and Title](#)

Muthuramalingam M, Dietz K-J, Ströher E (2010) Thiol–Disulfide Redox Proteomics in Plant Research. *NIH Public Access* 639: 1–14

Google Scholar: [Author Only](#) [Title Only](#) [Author and Title](#)

Naranjo B, Diaz-Espejo A, Lindahl M, Cejudo FJ (2016a) Type-f thioredoxins have a role in the short-term activation of carbon metabolism and their loss affects growth under short-day conditions in *Arabidopsis thaliana*. *J Exp Bot* 67: 1951–1964

Google Scholar: [Author Only](#) [Title Only](#) [Author and Title](#)

Naranjo B, Migné C, Krieger-Liszskay A, Hornero-Méndez D, Gallardo-Guerrero L, Cejudo FJ, Lindahl M (2016b) The chloroplast NADPH thioredoxin reductase C, NTRC, controls non-photochemical quenching of light energy and photosynthetic electron transport in *Arabidopsis*. *Plant Cell Environ* 39: 804–822

Google Scholar: [Author Only](#) [Title Only](#) [Author and Title](#)

Navrot N, Collin V, Gualberto J, Gelhaye E, Hirasawa M, Rey P, Knaff DB, Issakidis E, Jacquot JP, Rouhier N (2006) Plant glutathione peroxidases are functional peroxiredoxins distributed in several subcellular compartments and regulated during biotic and abiotic stresses. *Plant Physiol* 142: 1364–1379

Google Scholar: [Author Only](#) [Title Only](#) [Author and Title](#)

Niedermaier S, Schneider T, Bahl MO, Matsubara S, Huesgen PF (2020) Photoprotective Acclimation of the *Arabidopsis thaliana* Leaf Proteome to Fluctuating Light. *Front Genet* 11: 1–15

Google Scholar: [Author Only](#) [Title Only](#) [Author and Title](#)

Nikkanen L, Toivola J, Rintamäki E (2016) Crosstalk between chloroplast thioredoxin systems in regulation of photosynthesis. *Plant Cell Environ* 39: 1691–1705

Google Scholar: [Author Only](#) [Title Only](#) [Author and Title](#)

Nikkanen L, Toivola J, Trotta A, Manuel J, Diaz G, Tikkanen M, Aro E-M, Rintamäki E (2018) Regulation of cyclic electron flow by chloroplast NADPH-dependent thioredoxin system. doi: 10.1101/261560

Google Scholar: [Author Only](#) [Title Only](#) [Author and Title](#)

Ojeda V, Pérez-Ruiz JM, González M, Nájera VA, Sahrawy M, Serrato AJ, Geigenberger P, Cejudo FJ (2017) NADPH Thioredoxin Reductase C and Thioredoxins Act Concertedly in Seedling Development. *Plant Physiol* 174: 1436–1448

Google Scholar: [Author Only](#) [Title Only](#) [Author and Title](#)

Okegawa Y, Motohashi K (2015) Chloroplastic thioredoxin m functions as a major regulator of Calvin cycle enzymes during photosynthesis in vivo. *Plant Journal* 84: 900–913

Google Scholar: [Author Only](#) [Title Only](#) [Author and Title](#)

Okegawa Y, Motohashi K (2020) M-type thioredoxins regulate the PGR5/PGRL1-dependent pathway by forming a disulfide-linked complex with PGRL1. *Plant Cell* 32: 3866–3883

Google Scholar: [Author Only](#) [Title Only](#) [Author and Title](#)

Parker J, Balmant K, Zhu F, Zhu N, Chen S (2015) CysTMTRAQ - An integrative method for unbiased thiol-based redox proteomics. *Molecular and Cellular Proteomics* 14: 237–242

Google Scholar: [Author Only](#) [Title Only](#) [Author and Title](#)

Peled-Zehavi H, Avital S, Danon A (2010) Methods of redox signaling by plant thioredoxins. *Methods in redox signaling*

Google Scholar: [Author Only](#) [Title Only](#) [Author and Title](#)

Pérez-Pérez ME, Florencio FJ, Lindahl M (2006) Selecting thioredoxins for disulphide proteomics: target proteomes of three thioredoxins from the cyanobacterium *Synechocystis* sp. PCC 6803. *Proteomics* 6 Suppl 1: 186–195

Google Scholar: [Author Only](#) [Title Only](#) [Author and Title](#)

Pérez-Pérez ME, Mauriès A, Maes A, Tourasse NJ, Hamon M, Lemaire SD, Marchand CH (2017) The Deep Thioredoxome in *Chlamydomonas reinhardtii*: New Insights into Redox Regulation. *Mol Plant* 10: 1107–1125

Google Scholar: [Author Only](#) [Title Only](#) [Author and Title](#)

Pérez-Ruiz JM, Guinea M, Puerto-Galán L, Cejudo FJ (2014) NADPH Thioredoxin Reductase C Is Involved in Redox Regulation of the Mg-Chelatase I Subunit in *Arabidopsis thaliana* Chloroplasts. *Mol Plant* 7: 1252–1255

Google Scholar: [Author Only](#) [Title Only](#) [Author and Title](#)

Pérez-Ruiz JM, Naranjo B, Ojeda V, Guinea M, Cejudo FJ (2017) NTRC-dependent redox balance of 2-Cys peroxiredoxins is needed for optimal function of the photosynthetic apparatus. *Proceedings of the National Academy of Sciences* 114: 12069–12074

Google Scholar: [Author Only](#) [Title Only](#) [Author and Title](#)

Reichheld J-P, Khafif M, Riondet C, Droux M, Bonnard G, Meyer Y (2007) Inactivation of thioredoxin reductases reveals a complex interplay between thioredoxin and glutathione pathways in *Arabidopsis* development. *Plant Cell* 19: 1851–1865

Google Scholar: [Author Only](#) [Title Only](#) [Author and Title](#)

Richter AS, Peter E, Rothbart M, Schlicke H, Toivola J, Rintamäki E, Grimm B (2013) Posttranslational Influence of NADPH-

Dependent Thioredoxin Reductase C on Enzymes in Tetrapyrrole Synthesis. *Plant Physiol* 162: 63–73

Google Scholar: [Author Only](#) [Title Only](#) [Author and Title](#)

Scheibe R (1991) Redox-modulation of chloroplast enzymes: A common principle for individual control. *Plant Physiol* 96: 1–3

Google Scholar: [Author Only](#) [Title Only](#) [Author and Title](#)

Schjoerring JK, MäcK G, Nielsen KH, Husted S, Suzuki A, Driscoll S, Boldt R, Bauwe H (2006) Antisense reduction of serine hydroxymethyltransferase results in diurnal displacement of NH₄⁺ assimilation in leaves of *Solanum tuberosum*. *Plant Journal* 45: 71–82

Google Scholar: [Author Only](#) [Title Only](#) [Author and Title](#)

Schürmann P, Buchanan BB (2008) The ferredoxin/thioredoxin system of oxygenic photosynthesis. *Antioxid Redox Signal* 10: 1235–74

Google Scholar: [Author Only](#) [Title Only](#) [Author and Title](#)

Selinski J, Scheibe R (2019) Malate valves: old shuttles with new perspectives. *Plant Biol* 21: 21–30

Google Scholar: [Author Only](#) [Title Only](#) [Author and Title](#)

Serrato AJ, Pérez-Ruiz JM, Spínola MC, Cejudo FJ (2004) A novel NADPH thioredoxin reductase, localized in the chloroplast, which deficiency causes hypersensitivity to abiotic stress in *Arabidopsis thaliana*. *J Biol Chem* 279: 43821–43827

Google Scholar: [Author Only](#) [Title Only](#) [Author and Title](#)

Shin JS, Kim SY, So WM, Noh M, Yoo KS, Shin JS (2020) Lon domain-containing protein 1 represses thioredoxin y2 and regulates ROS levels in *Arabidopsis* chloroplasts. *FEBS Lett* 594: 986–994

Google Scholar: [Author Only](#) [Title Only](#) [Author and Title](#)

Simionato D, Basso S, Zaffagnini M, Lana T, Marzotto F, Trost P, Morosinotto T (2015) Protein redox regulation in the thylakoid lumen: The importance of disulfide bonds for violaxanthin de-epoxidase. *FEBS Lett* 589: 919–923

Google Scholar: [Author Only](#) [Title Only](#) [Author and Title](#)

Somerville CR, Ogren WL (1980) Inhibition of photosynthesis in. *Nature* 286: 257–259

Google Scholar: [Author Only](#) [Title Only](#) [Author and Title](#)

Stöcker S, Maurer M, Ruppert T, Dick TP (2018) A role for 2-Cys peroxiredoxins in facilitating cytosolic protein thiol oxidation. *Nat Chem Biol* 14: 148–155

Google Scholar: [Author Only](#) [Title Only](#) [Author and Title](#)

Suzuki A, Knaff DB (2005) Glutamate synthase: Structural, mechanistic and regulatory properties, and role in the amino acid metabolism. *Photosynth Res* 83: 191–217

Google Scholar: [Author Only](#) [Title Only](#) [Author and Title](#)

Teh JT, Leitz V, Holzer VJC, Neusius D, Marino G, Meitzel T, García-Cerdán JG, Dent RM, Niyogi KK, Geigenberger P, et al (2023) NTRC regulates CP12 to activate Calvin–Benson cycle during cold acclimation. *Proceedings of the National Academy of Sciences*. doi: 10.1073/pnas.2306338120

Google Scholar: [Author Only](#) [Title Only](#) [Author and Title](#)

Thormählen I, Meitzel T, Groysman J, Öchsner AB, von Roepenack-Lahaye E, Naranjo B, Cejudo FJ, Geigenberger P (2015) Thioredoxin f1 and NADPH-dependent thioredoxin reductase C have overlapping functions in regulating photosynthetic metabolism and plant growth in response to varying light conditions. *Plant Physiol* 169: pp.01122.2015

Google Scholar: [Author Only](#) [Title Only](#) [Author and Title](#)

Thormählen I, Ruber J, Von Roepenack-Lahaye E, Ehrlich SM, Massot V, Hümmer C, Tezycka J, Issakidis-Bourguet E, Geigenberger P (2013) Inactivation of thioredoxin f1 leads to decreased light activation of ADP-glucose pyrophosphorylase and altered diurnal starch turnover in leaves of *Arabidopsis* plants. *Plant Cell Environ* 36: 16–29

Google Scholar: [Author Only](#) [Title Only](#) [Author and Title](#)

Thormählen I, Zupok A, Rescher J, Leger J, Weissenberger S, Groysman J, Orwat A, Chatel-Innocenti G, Issakidis-Bourguet E, Armbruster U, et al (2017) Thioredoxins Play a Crucial Role in Dynamic Acclimation of Photosynthesis in Fluctuating Light. *Mol Plant* 10: 168–182

Google Scholar: [Author Only](#) [Title Only](#) [Author and Title](#)

Topf U, Suppanz I, Samluk L, Wrobel L, Böser A, Sakowska P, Knapp B, Pietrzyk MK, Chacinska A, Warscheid B (2018) Quantitative proteomics identifies redox switches for global translation modulation by mitochondrially produced reactive oxygen species. *Nat Commun*. doi: 10.1038/s41467-017-02694-8

Google Scholar: [Author Only](#) [Title Only](#) [Author and Title](#)

Uhrig RG, Echevarría-Zomeño S, Schlapfer P, Grossmann J, Roschitzki B, Koerber N, Fiorani F, Grisse W (2021) Diurnal dynamics of the *Arabidopsis* rosette proteome and phosphoproteome. *Plant Cell Environ* 44: 821–841

Google Scholar: [Author Only](#) [Title Only](#) [Author and Title](#)

- Vaseghi M-J, Chibani K, Telman W, Liebthal MF, Gerken M, Schnitzer H, Mueller SM, Dietz K-J (2018) The chloroplast 2-cysteine peroxiredoxin functions as thioredoxin oxidase in redox regulation of chloroplast metabolism. *Elife*. doi: 10.7554/eLife.38194
Google Scholar: [Author Only](#) [Title Only](#) [Author and Title](#)
- Wang P, Liu J, Liu B, Da Q, Feng D, Su J, Zhang Y, Wang J, Wang H bin (2014) Ferredoxin:Thioredoxin reductase is required for proper chloroplast development and is involved in the regulation of plastid gene expression in *Arabidopsis thaliana*. *Mol Plant* 7: 1586–1590
Google Scholar: [Author Only](#) [Title Only](#) [Author and Title](#)
- Wang P, Liu J, Liu B, Feng D, Da Q, Wang P, Shu S, Su J, Zhang Y, Wang J, et al (2013) Evidence for a role of chloroplastic m-type thioredoxins in the biogenesis of photosystem II in *Arabidopsis*. *Plant Physiol* 163: 1710–1728
Google Scholar: [Author Only](#) [Title Only](#) [Author and Title](#)
- Wittmann D, Geigenberger P, Grimm B (2023) NTRC and TRX-f Coordinately Affect the Levels of Enzymes of Chlorophyll Biosynthesis in a Light-Dependent Manner. *Cells* 12: 1670
Google Scholar: [Author Only](#) [Title Only](#) [Author and Title](#)
- Wong JH, Cai N, Balmer Y, Tanaka CK, Vensel WH, Hurkman WJ, Buchanan BB (2004) Thioredoxin targets of developing wheat seeds identified by complementary proteomic approaches. *Phytochemistry* 65: 1629–1640
Google Scholar: [Author Only](#) [Title Only](#) [Author and Title](#)
- Yamamoto HY, Kamite L (1972) The effects of dithiothreitol on violaxanthin de-epoxidation and absorbance changes in the 500-nm region. *Biochimica et Biophysica Acta (BBA) - Bioenergetics* 267: 538–543
Google Scholar: [Author Only](#) [Title Only](#) [Author and Title](#)
- Yamazaki D, Motohashi K, Kasama T, Hara Y, Hisabori T (2004) Target Proteins of the Cytosolic Thioredoxins in *Arabidopsis thaliana*. *Plant Cell Physiol* 45: 18–27
Google Scholar: [Author Only](#) [Title Only](#) [Author and Title](#)
- Yano H, Wong JH, Lee YM, Cho MJ, Buchanan BB (2001) A strategy for the identification of proteins targeted by thioredoxin. *Proc Natl Acad Sci U S A* 98: 4794–4799
Google Scholar: [Author Only](#) [Title Only](#) [Author and Title](#)
- Yoshida K, Hara S, Hisabori T (2015) Thioredoxin selectivity for thiol-based redox regulation of target Proteins in Chloroplasts. *Journal of Biological Chemistry* 290: 14278–14288
Google Scholar: [Author Only](#) [Title Only](#) [Author and Title](#)
- Yoshida K, Hisabori T (2016) Two distinct redox cascades cooperatively regulate chloroplast functions and sustain plant viability. *Proceedings of the National Academy of Sciences* 113: E3967–E3976
Google Scholar: [Author Only](#) [Title Only](#) [Author and Title](#)
- Yoshida K, Noguchi K, Motohashi K, Hisabori T (2013) Systematic exploration of thioredoxin target proteins in plant mitochondria. *Plant Cell Physiol* 54: 875–892
Google Scholar: [Author Only](#) [Title Only](#) [Author and Title](#)
- Yoshida K, Yokochi Y, Tanaka K, Hisabori T (2022) The ferredoxin/thioredoxin pathway constitutes an indispensable redox-signaling cascade for light-dependent reduction of chloroplast stromal proteins. *Journal of Biological Chemistry* 298: 102650
Google Scholar: [Author Only](#) [Title Only](#) [Author and Title](#)
- Yu A, Xie Y, Pan X, Zhang H, Cao P, Su X, Chang W, Li M (2020) Photosynthetic Phosphoribulokinase Structures: Enzymatic Mechanisms and the Redox Regulation of the Calvin-Benson-Bassham Cycle. *Plant Cell* 32: 1556–1573
Google Scholar: [Author Only](#) [Title Only](#) [Author and Title](#)
- Zaffagnini M, Fermani S, Marchand CH, Costa A, Sparla F, Rouhier N, Geigenberger P, Lemaire SD, Trost P (2019) Redox Homeostasis in Photosynthetic Organisms: Novel and Established Thiol-Based Molecular Mechanisms. *Antioxid Redox Signal* 31: 155–210
Google Scholar: [Author Only](#) [Title Only](#) [Author and Title](#)
- Zimmer D, Swart C, Graf A, Arrivault S, Tillich M, Proost S, Nikoloski Z, Stitt M, Bock R, Mühlhaus T, et al (2021) Topology of the redox network during induction of photosynthesis as revealed by time-resolved proteomics in tobacco. *Sci Adv*. doi: 10.1126/sciadv.abi8307
Google Scholar: [Author Only](#) [Title Only](#) [Author and Title](#)